JOURNAL OF GEOPHYSICAL RESEARCH, VOL. 85, NO. B11, PAGES 6479–6495, NOVEMBER 10, 1980

Seismicity and Tectonic Stress in the South-Central Pacific

ÉMILE A. OKAL

Department of Geology and Geophysics, Yale University, New Haven, Connecticut 06520

JACQUES TALANDIER

Laboratoire de Géophysique, Commissariat à l'Energie Atomique, Papeete, Tahiti

KEITH A. SVERDRUP AND THOMAS H. JORDAN

Geological Research Division, Scripps Institution of Oceanography, La Jolla, California 92093

The 15-station French Polynesian Seismic Network is used to study the intraplate seismicity of the South-Central Pacific Ocean for the period January 1, 1965 to December 31, 1979. The overall pattern of seismicity shows a clustering of earthquakes at approximately 30 distinct localities, occurring both as discrete events and in swarms. Three localities are associated with known centers of active vulcanism (Moua Pihaa and Rocard seamounts in the Tahiti-Méhétia area and Macdonald seamount in the Austral Islands). A set of eight localities is distributed along the tectonic axis of the Tuamotu Archipelago and its northwestward extention into the Line Islands, and a set of five is roughly aligned with the northeastern edge of the Tuamotu platform; both sets may be related to load inhomogeneities in the lithosphere. However, much of the seismicity is not correlated with major bathymetric features. With the exception of one isolated event, for example, none of the recorded activity occurs along the major fracture zones that cross the study area.

Only three localities have been the sites of two or more earthquakes with body-wave magnitudes greater than 5.0; these we designate Regions A, B and C. Excluding Hawaii, Regions A, B and C are the most intense centers of seismicity within the Pacific plate interior, and together they account for more than 90% of the seismic energy release in the South-Central Pacific. An analysis of water multiples from events in Regions A, B and C indicates hypocentral depths within the oceanic crust. Eight focal mechanisms have been obtained; these all have nearly horizontal, NW-trending compressional axes, oriented approximately parallel to the direction of Pacific plate motion. The uniformity of this orientation over the large distances separating the epicenters (>2000 km) suggests that the mechanisms are indicative of a regional tectonic stress field, rather than locally disturbed stress patterns. These data thus provide additional constraints on the force balance models of plate tectonics.

INTRODUCTION

Over the last decade and a half, the many studies of seismicity and focal mechanisms at plate boundaries have provided information essential to the description of present-day plate kinematics [*Sykes*, 1967; *Isacks et al.*, 1968; *Minster and Jordan*, 1978]. More attention is now being focused on intraplate earthquakes—those occurring far from the plate boundaries—in attempts to characterize the state of stress within the lithosphere and thereby constrain plate dynamics. It has been found in a number of instances that the compressional axes of intraplate focal mechanisms are nearly horizontal and approximately parallel to the directions of plate motion away from the ridge crests [*Mendiguren*, 1971; *Sykes and Sbar*, 1974; *Forsyth*, 1973; *Mendiguren and Richter*, 1978; *Okal*, 1980]. To satisfy these data evidently requires a model of plate dynamics in which the gravitational body forces associated with the horizontal density gradients near spreading centers ('ridge push' forces) play a significant role [*Forsyth and Uyeda*, 1975; *Solomon et al.*, 1975; *Richardson et al.*, 1976, 1979].

The interpretation of focal mechanisms in terms of driving forces is not without complications, however. There exist other sources of lithospheric stress large enough to fracture rocks, including load inhomogeneities, lithospheric cooling, and changes in plate curvature due to latitudinal motion on an ellipsoidal earth [*Turcotte and Oxburgh*, 1973, 1976], and the influence of these stresses on the seismic data must be evaluated. Furthermore, pre-existing zones of weakness, such as old faults and fracture zones, are often the preferential sites for intraplate seismicity [*Sykes*, 1978], and the role of these local structures in distorting the ambient stress field has not been completely assessed, especially in continental environments. In fact, the continental cratons may themselves distort the large-scale stress field of the plates [*Wesnousky and Scholz*, 1980].

Unfortunately, most detailed studies of intraplate seismicity and stress-field orientation have been confined to continental areas, where the seismic activity is higher and where extensive instrument networks provide better regional coverage. In oceanic regions only large isolated events have been examined, and rarely are the data sufficient to yield accurate orientations of both nodal planes [e.g., *Mendiguren*, 1971]. Hence, the constraints on the tectonic stress field in the oceans are few, particularly in the Pacific, as emphasized in a recent review by *Richardson et al.* [1979].

The existence of a 15-station network of short period seismometers in French Polynesia has provided the opportunity for a detailed regional investigation of the seismicity of the South-Central Pacific Ocean. *Talandier and Kuster* [1976], in a previous study using this network, concentrated their interest on the Tahiti-Méhétia (TM) area (16°–19°S, 147°–150°W). Their work revealed the existence of two active submarine volcanoes less than 100 km southeast of Tahiti, evidently

Paper number 80B0922.
0148-0227/80/080B-0922$01.00

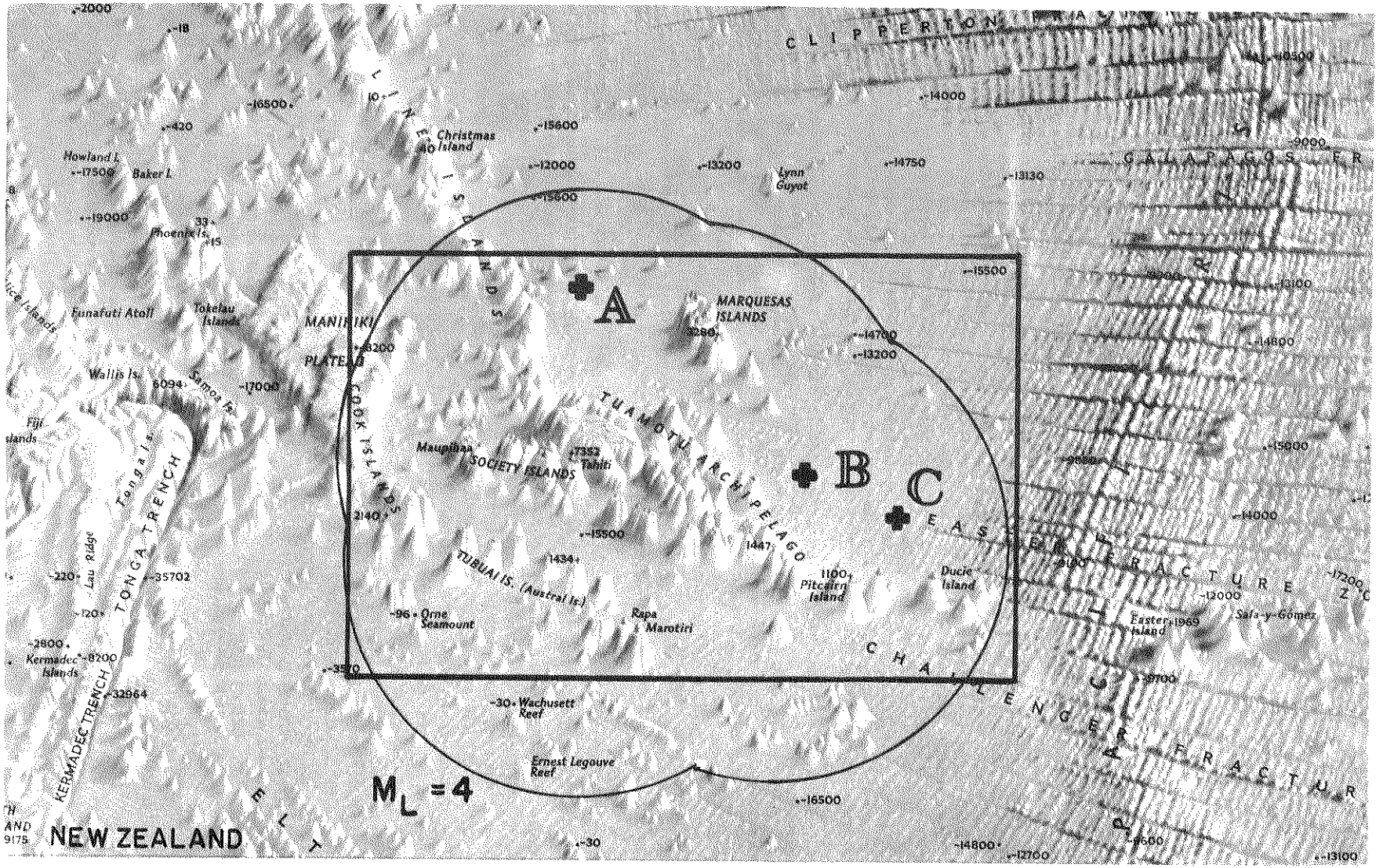

Fig. 1. Generalized physiographic map of the Pacific Ocean (reproduced by permission of the National Geographic Society). Light arcs delimit the region within the $M_L = 4$ detection threshold of the French Polynesian Network. Area outlined by heavy box is shown in Figure 3. Seismic Regions A, B and C are indicated by crosses.

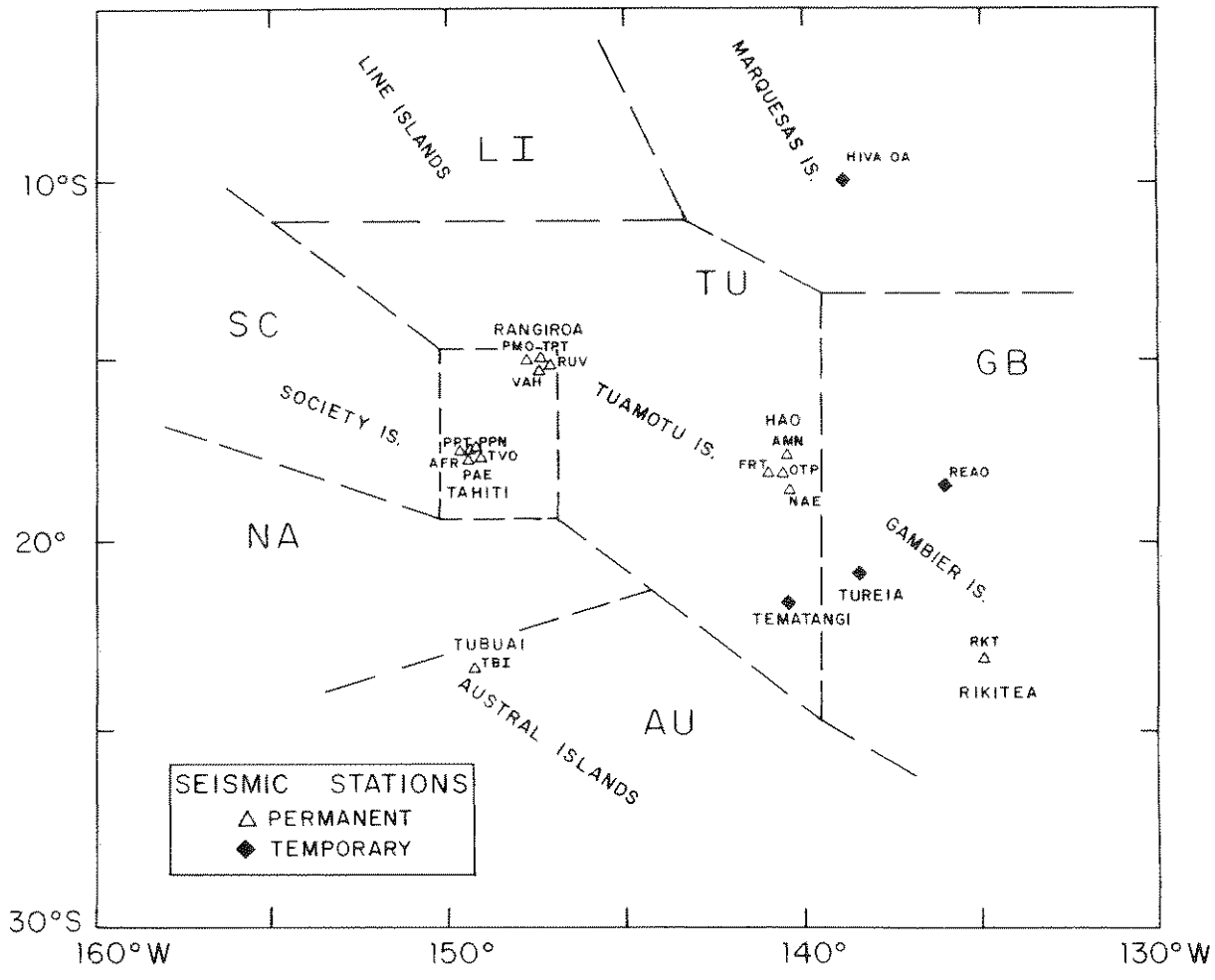

Fig. 2. Locations of the permanent and temporary stations comprising the French Polynesian Network. Seismic zones discussed in the text are identified by two-letter codes.

marking a hotspot associated with the Society Island chain.

This paper extends these investigations to the entire area covered by the French Polynesian Network for the period January 1, 1965, to December 31, 1979 (Figures 1 and 2). The overall pattern of seismicity shows a clustering of earthquakes at approximately 30 distinct localities (Figure 3), occurring both as discrete events and in swarms. We examine in greater detail the activity at three of these localities, designated Regions A, B and C (Figure 1), which together account for more than 90% of the seismic energy released in the South-Central Pacific and which are the most intense centers of seismicity within the Pacific plate interior, excluding Hawaii. Focal mechanisms are obtained for nine larger events ($4.9 \leq m_b \leq 5.5$); eight of these have nearly horizontal, NW-trending compressional axes oriented approximately parallel to the direction of Pacific plate motion. The uniformity of this orientation over a distance in excess of 2000 km suggests that the mechanisms are indicative of a regional tectonic stress field, rather than locally disturbed stress patterns.

SEISMICITY

The area under study is delineated by the box on the physiographic map of Figure 1; it extends from 5°S to 30°S and from 120°W to 160°W. As shown by the figure, most of the area lies within the magnitude-4 detection threshold of the French Polynesian Network. The seismometer stations constituting this network are listed in Table 1 and located on Figure 2. There is a 5-station array on Tahiti and Mooréa in the Society Islands and two 4-station arrays, one on Rangiroa and the other on Hao and Amanu, in the Tuamotu Archipelago. Each array has an aperture of about 50 km. In addition, there are isolated permanent stations at Tubuai in the Austral Islands and Rikitéa in the Gambier Islands, as well as a number of temporary stations operated at various times on various atolls (Figure 2). Special instrumentation permits magnifications of up to 10^5 at 1 Hz and up to 2×10^6 at 3 Hz [*Talandier*, 1971; *Talandier and Kuster*, 1976]; the gains are considerably greater than for standard installations on oceanic islands (typically 10^4 or less at 1 Hz).

Network installation was not completed until 1976, so the detection capabilities of the network are a function of time. For example, a considerable increase in the area covered by the $M_L = 3$ detection threshold resulted from the implementation of station TBI and the Hao array in 1976. At the $M_L = 4$ level, however, the network coverage has increased only slightly since 1967, when RKT and three stations on Rangiroa were installed, and most of this increase is confined to the extreme northeastern and southwestern parts of the study area, where no seismicity has yet been detected.

The seismicity of the study region for the period January 1, 1965, to December 31, 1979, is listed in Tables 2 and 3 and plotted on Figures 3 and 4. Several techniques were used to

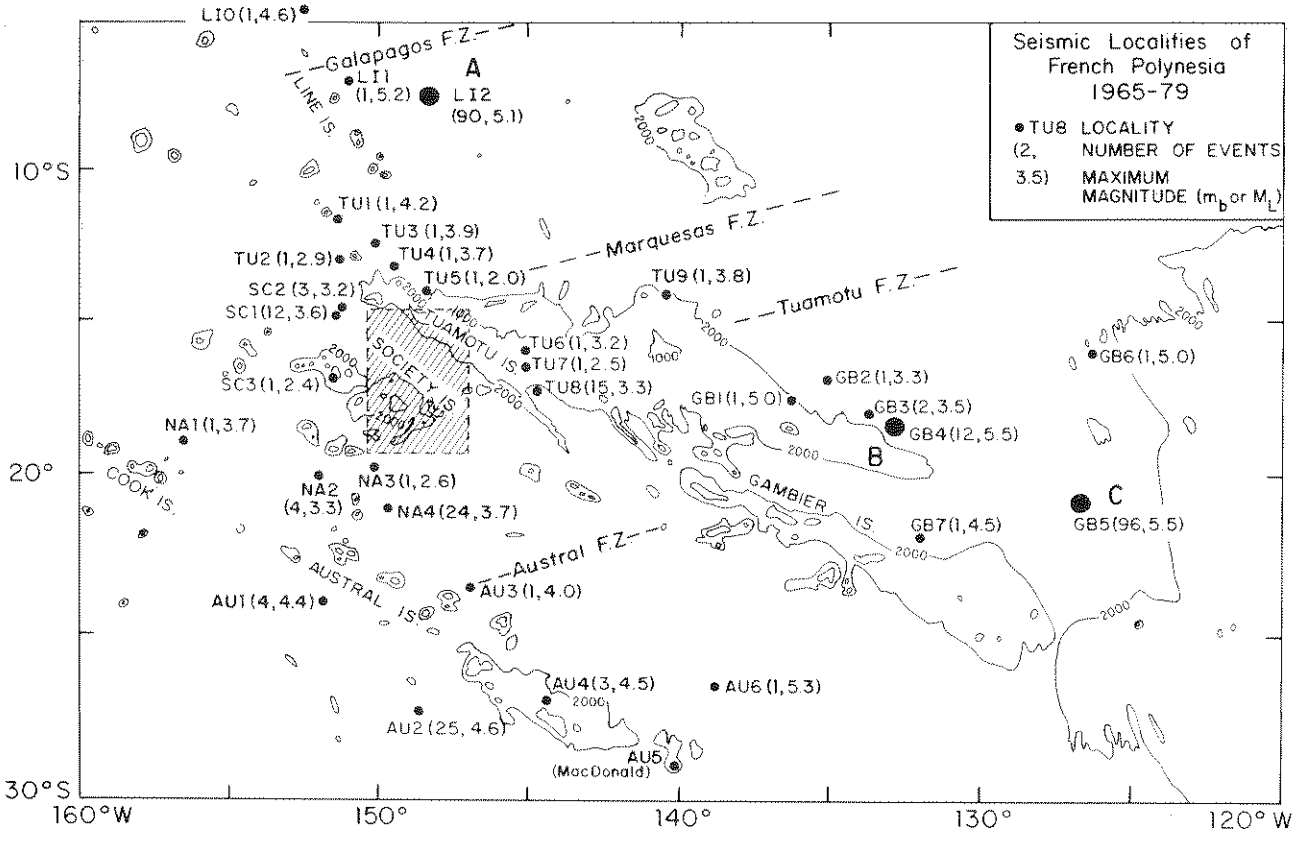

Fig. 3. Seismic localities in the South-Central Pacific, as designated in Table 2. Epicenters in the Tahiti-Méhétia area (hatched box) have been omitted; these are plotted in Figure 4. Total number of observed events and maximum recorded magnitude are indicated in parentheses. 1000 and 2000 fathom contours after *Mammerickx et al.* [1975].

obtain the locations. For most events with $m_b \geq 4.4$, locations were determined by the United States Geological Survey (USGS) or the International Seismological Centre (ISC). Epicenters derived by these agencies are labelled *T*, for teleseismic, in Table 2, with the USGS location being used in instances where both were available.

Errors are introduced into the teleseismic locations by several factors, including poor station coverage at distances less than 50°, the lack of depth control, and the use of continental crustal models in the location routines. Because of these problems, hypocentral depths of 33 km were assigned to most of the teleseismic locations by both the USGS and the ISC, although this value is particularly meaningless in the oceanic environment. Location errors are often apparent in the P_n times computed for stations in French Polynesia. The USGS location for the May 25, 1975, earthquake, for example, implies a P_n velocity of 7.3 km/s for a path to the temporary station on Réao, which is much lower than the regional values determined by *Talandier and Bouchon* [1979].

A number of the larger events have therefore been relocated; these are labelled *R* in Table 2. In the relocation experiments the hypocentral depths were constrained to be 5 km below the sediment-water interface; such shallow hypocenters are consistent with our observations of surface-reflected phases discussed in the next section. The May 25, 1975, event, occurring in Region B and extensively recorded in French Polynesia, was relocated with a restricted set of teleseismic stations, well distributed azimuthally, plus a complete set of

TABLE 1. Seismic Stations of the French Polynesian Network

Code	Name	Island	Archipelago	Latitude, °S	Longitude, °W	Geological Setting	Start Date
AFR	Afaréaitu	Mooréa	Society	17.538	149.777	volcanic	1962
PAE	Paea	Tahiti	Society	17.662	149.580	volcanic	1962
PPT	Pamatai	Tahiti	Society	17.569	149.576	volcanic	1962
PPN	Papenoo	Tahiti	Society	17.531	149.432	volcanic	1965
TVO	Taravao	Tahiti	Society	17.782	149.252	volcanic	1966
PMO	Pomariorio	Rangiroa	Tuamotu	15.004	147.897	atoll	1967
VAH	Vaihoa	Rangiroa	Tuamotu	15.239	147.631	atoll	1967
TPT	Tiputa	Rangiroa	Tuamotu	14.984	147.620	atoll	1967
RUV	Rauvai	Rangiroa	Tuamotu	15.189	147.384	atoll	1971
RKT	Rikitéa	Mangaréva	Gambier	23.120	134.973	volcanic	1966
TBI	Tubuai	Tubuai	Austral	23.349	149.461	volcanic	1976
FRT	Faratahi	Hao	Tuamotu	18.170	141.042	atoll	1976
OTP	Otepa	Hao	Tuamotu	18.167	140.857	atoll	1976
NAE	Nake	Nao	Tuamotu	18.424	140.669	atoll	1976
AMN	Amanu	Amanu	Tuamotu	17.851	140.859	atoll	1976

TABLE 2. Seismicity of the South-Central Pacific, 1965–1979 (Tahiti-Méhétia Area Excluded)

DATE	ORIGIN TIME	EPICENTER		LOCATION	MAG	ID
Y M D	H M S	S	W			
	LI LINE ISLANDS					
CI0						
62 01 25	10 03 06.8	4.6	152.6	T	4.6	
LI1						
67 04 13	14 26 49.5	7.0	151.0	T	5.2	
LI2 ******	REGION A ******					
68 06 02	20 26 41	7.4	148.0	L	3.6	
68 06 07	20 14 47	7.4	148.0	L	3.7	
68 07 29	02 45 44.5	7.50	148.27	R	4.9	*A1
68 08 02	23 58 06	7.4	148.0	L	4.0	
68 09 14	08 04 23	7.4	148.0	L	3.7	
68 09 14	16 34 08	7.4	148.0	L	4.0	
68 10 03	12 14 03	7.4	148.0	L	3.9	
68 10 08	22 58 04.3	7.20	148.16	T	4.4	
68 10 10	01 04 35.1	7.60	148.10	T	4.4	
68 11 23	00 13 35.3	7.62	148.13	T	4.6	
68 12 27	11 00 38	7.4	148.0	L	4.2	
68 12 28	01 11 22	7.4	148.0	L	4.0	
68 12 28	20 03 04.7	7.60	148.60	T	4.7	
69 01 17	19 24 04	7.4	148.0	L	3.8	
69 01 20	20 16 24	7.4	148.0	L	3.9	
69 04 03	19 41 29	7.4	148.0	L	4.0	
69 04 09	19 47 35	7.4	148.0	L	3.6	
69 04 10	00 02 12	7.4	148.0	L	3.6	
69 04 17	02 04 29	7.4	148.0	L	3.6	
69 05 27	21 02 28	7.4	148.0	L	3.8	
69 05 27	06 28 28	7.4	148.0	L	3.7	
69 05 27	22 23 24	7.4	148.0	L	3.4	
69 06 01	03 35 30.2	7.66	148.20	T	4.4	
69 06 02	15 53 49	7.4	148.0	L	3.9	
69 06 02	16 14 55	7.4	148.0	L	3.7	
69 06 06	16 34 53.7	7.60	148.40	T	4.5	
69 06 06	16 43 17	7.4	148.0	L	3.6	
69 06 06	16 43 32	7.4	148.0	L	3.6	
69 06 06	16 43 52	7.4	148.0	L	3.8	
69 06 06	16 51 48	7.4	148.0	L	3.2	
69 06 06	17 53 38.5	7.70	148.00	T	4.6	
69 06 15	07 56 09	7.4	148.0	L	3.6	
69 07 04	12 20 34	7.4	148.0	L	4.0	
69 07 24	09 58 15	7.4	148.0	L	3.6	
69 07 24	09 29 53	7.4	148.0	L	3.6	
69 07 24	19 17 11	7.4	148.0	L	4.1	
69 07 24	22 55 30	7.4	148.0	L	3.6	
69 07 25	21 33 16	7.4	148.0	L	4.1	
69 08 02	01 42 50	7.4	148.0	L	4.2	
69 08 02	12 53 25	7.4	148.0	L	3.8	
69 08 06	17 15 39.7	7.36	148.38	R	5.1	*A2
69 08 06	20 36 24	7.4	148.0	L	3.7	
69 08 06	21 12 32	7.4	148.0	L	3.6	
69 08 06	21 19 03	7.4	148.0	L	3.6	
69 08 06	21 22 17	7.4	148.0	L	3.5	
69 08 07	00 40 54	7.4	148.0	L	3.8	
69 08 09	13 38 45	7.4	148.0	L	3.8	
69 08 24	20 14 13	7.4	148.0	L	4.1	
69 09 07	04 52 22	7.4	148.0	L	4.0	
69 09 30	18 50 20	7.4	148.0	L	4.0	
69 09 30	19 21 25	7.4	148.0	L	3.7	
69 11 06	17 05 17	7.4	148.0	L	4.1	
69 11 10	23 14 01	7.4	148.0	L	4.3	
70 02 22	22 51 49	7.4	148.0	L	3.9	
70 02 22	23 56 58	7.4	148.0	L	4.0	
70 04 19	00 06 24	7.4	148.0	L	4.5	
70 04 19	01 47 22	7.4	148.0	L	4.7	
70 04 19	04 56 02	7.4	148.0	L	3.7	
70 04 19	05 57 25	7.4	148.0	L	3.8	
70 04 19	06 55 16	7.4	148.0	L	3.9	
70 04 19	08 34 06	7.4	148.0	L	3.7	
70 04 19	10 37 01	7.4	148.0	L	3.5	
70 04 19	04 22 52	7.4	148.0	L	3.9	
70 04 19	12 32 58.2	7.66	148.80	T	4.6	
70 04 20	18 58 26	7.4	148.0	L	3.5	
70 04 20	19 25 44	7.4	148.0	L	3.5	
72 02 06	04 55 57	7.4	148.0	L	3.8	
73 01 19	07 36 32.9	7.37	148.28	R	4.9	*A3
73 01 19	13 41 43	7.4	148.0	L	3.8	
73 01 19	13 41 53	7.4	148.0	L	4.0	
73 01 19	13 49 32	7.4	148.0	L	3.5	
73 01 19	13 58 23	7.4	148.0	L	3.5	
73 01 19	13 58 37	7.4	148.0	L	3.9	
73 01 19	14 19 11.8	7.50	148.30	T	4.4	
73 01 19	15 26 26.1	7.22	146.35	R	4.9	*A4
73 01 19	15 56 24.2	7.60	148.30	T	4.6	
73 01 27	22 14 58	7.4	148.0	L	3.7	
74 06 16	09 08 26	7.4	148.0	L	3.7	
74 10 31	02 58 46	7.4	148.0	L	3.9	
74 10 31	02 55 17	7.4	148.0	L	3.3	
75 06 19	12 33 24	7.4	148.0	L	3.4	
76 01 15	23 05 50	7.4	148.0	L	3.5	
76 06 30	20 25 51	7.4	148.0	L	4.0	
76 16 24	06 33 09	7.4	148.0	L	3.8	
76 10 24	14 22 00	7.4	148.0	L	3.7	
76 10 24	14 22 35	7.4	148.0	L	4.1	
76 10 24	14 22 56	7.4	148.0	L	3.7	
76 10 24	14 24 53	7.4	148.0	L	3.7	
76 10 25	03 50 59	7.4	148.0	L	3.6	
76 10 25	04 00 31	7.4	148.0	L	3.2	
	TU WESTERN TUAMOTU ISLANDS					
TU1						
66 03 27	04 26 43	11.7	151.4	L	4.2	
TU2						
77 12 24	11 08 11	13.0	151.3	L	2.9	
TU4						
77 03 04	22 00 15	12.5	150.2	L	3.9	
TU8						
72 11 21	16 18 33	13.3	149.5	L	3.7	
TU5						
74 01 18	08 01 56	14.1	148.4	L	2.0	
TU6						
74 12 02	17 23 36	16.0	145.1	L	3.2	
TU7						
75 06 10	19 35 12	16.6	145.1	L	2.5	
TU8						
76 09 24	10 29 39	17.3	144.7	L	3.1	
76 10 05	21 00 49	17.3	144.7	L	2.7	
76 10 06	06 58 17	17.3	144.7	L	2.7	
76 10 07	02 06 24	17.3	144.7	L	2.4	
76 10 09	21 35 52	17.3	144.7	L	2.4	
76 10 10	03 48 41	17.3	144.7	L	2.7	
76 10 10	04 09 23	17.3	144.7	L	2.8	
76 10 10	13 18 13	17.3	144.7	L	3.3	
76 10 16	05 27 06	17.3	144.7	L	2.7	
76 10 23	08 57 26	17.3	144.7	L	2.7	
76 10 23	11 30 11	17.3	144.7	L	2.4	
76 11 01	12 06 00	17.3	144.7	L	3.1	
76 12 12	03 55 32	17.3	144.7	L	2.3	
77 01 10	17 13 38	17.3	144.7	L	2.3	
77 04 26	10 37 01	17.3	144.7	L	2.4	
TU9						
79 02 13	12 36 59	14.2	140.5	L	3.8	
	SC NORTHWEST OF SOCIETY ISLANDS					
SC1						
69 07 18	08 01 21	14.9	151.4	L	2.4	
69 09 27	16 28 52	14.9	151.4	L	2.5	
72 03 31	17 33 26	14.9	151.4	L	3.8	
72 10 10	04 23 48	14.9	151.4	L	3.1	
73 05 12	05 53 02	14.9	151.4	L	2.6	
73 05 12	08 31 56	14.9	151.4	L	2.5	
73 07 18	09 14 52	14.9	151.4	L	2.5	
74 05 05	01 08 57	14.9	151.4	L	2.6	
75 06 10	09 28 25	14.9	151.4	L	2.1	
76 03 20	07 06 57	14.9	151.4	L	2.6	
77 09 11	00 06 01	14.9	151.4	L	2.3	
78 03 06	02 43 46	14.9	151.4	L	2.4	
SC2						
71 08 14	21 31 55	14.7	151.3	L	2.1	
71 09 10	11 13 19	14.7	151.3	L	3.2	
74 02 14	17 07 55	14.7	151.3	L	2.5	
SC3						
79 11 14	08 02 49	16.7	151.4	L	2.4	
	NA COOK ISLANDS AND NORTH OF AUSTRAL ISLANDS					
NA1						
68 04 01	14 56 34	19.0	156.5	L	3.7	
NA2						
68 10 08	17 17 12.2	20.1	152.8	L	3.3	
73 12 21	10 00 00	20.1	152.8	L	2.3	
74 05 15	16 56 07	20.1	152.0	L	2.5	
75 09 07	02 12 24	20.1	152.0	L	2.8	
NA3						
76 05 15	09 58 43	19.8	150.1	L	2.6	
NA4						
74 08 18	07 34 25	21.1	149.6	L	2.2	
74 09 29	05 04 18	21.1	149.6	L	2.8	
75 01 20	03 42 46	21.1	149.6	L	2.9	
75 05 22	05 56 45	21.1	149.6	L	3.0	
75 06 06	20 05 13	21.1	149.6	L	2.4	
75 07 30	02 37 48	21.1	149.6	L	2.3	
75 10 16	09 07 28	21.1	149.6	L	2.4	
75 11 15	20 34 47	21.1	149.6	L	3.4	
75 11 16	10 13 46	21.1	149.6	L	2.9	
75 12 02	12 11 43	21.1	149.6	L	2.7	
76 03 15	21 54 27	21.1	149.6	L	2.7	
76 05 12	02 30 26	21.1	149.6	L	3.2	
77 05 20	13 43 05	21.1	149.6	L	2.6	
77 05 24	06 06 54	21.1	149.6	L	2.8	
77 07 29	02 13 18	21.1	149.6	L	2.8	
77 08 27	01 08 36	21.1	149.6	L	2.7	
77 09 07	14 23 46	21.1	149.6	L	2.6	
77 09 13	03 13 53	21.1	149.6	L	2.4	
77 11 02	03 38 55	21.1	149.6	L	2.8	
77 12 22	05 58 59	21.1	149.6	L	2.8	
78 08 05	09 49 45	21.1	149.6	L	2.8	
78 04 14	09 19 48	21.1	149.6	L	2.9	
78 10 14	13 07 00	21.1	149.6	L	3.3	
78 10 18	23 54 20	21.1	149.6	L	3.3	
	AU AUSTRAL ISLANDS					
AU1						
70 02 03	14 47 51	24.1	151.8	L	3.5	
70 05 28	16 31 53	24.1	151.8	L	3.5	
70 08 04	11 32 23	24.1	151.8	L	4.6	
70 08 13	12 04 31	24.1	151.8	L	4.4	
AU2						
70 05 14	09 35 52	27.4	148.6	L	4.5	
77 04 24	16 31 03	27.4	148.6	L	3.4	
77 05 20	20 30 52	27.4	148.6	L	3.3	
77 06 28	03 37 01	27.4	148.6	L	4.1	
77 06 29	05 27 41	27.4	148.6	L	3.6	
77 09 16	16 08 46	27.4	148.6	L	3.1	
77 09 20	12 33 48	27.4	148.6	L	3.9	
77 10 12	19 09 17	27.4	148.6	L	3.2	
77 10 28	02 27 29	27.4	148.6	L	3.2	
77 11 15	18 57 16	27.4	148.6	L	4.6	
78 01 31	11 10 06	27.4	148.6	L	3.9	
78 02 14	01 33 26	27.4	148.6	L	3.7	
78 03 08	10 18 26	27.4	148.6	L	3.7	
78 03 25	04 44 09	27.4	148.6	L	3.1	
78 03 31	23 49 24	27.4	148.6	L	3.7	
78 05 05	13 29 08	27.4	148.6	L	3.8	
78 05 21	07 12 17	27.4	148.6	L	3.7	
78 06 08	20 40 00	27.4	148.6	L	3.3	
78 06 09	16 54 04	27.4	148.6	L	3.3	
78 06 09	12 06 46	27.4	148.6	L	3.3	
78 06 10	12 01 15	27.4	148.6	L	3.2	
78 06 10	13 19 53	27.4	148.6	L	3.4	
78 06 12	01 09 11	27.4	148.6	L	3.0	
78 06 12	15 01 58	27.4	148.6	L	3.9	
78 06 16	02 36 56	27.4	149.0	L	3.6	
AU3						
72 01 13	17 48 27	23.6	146.9	L	4.0	
AU4						
77 03 12	17 31 00	22.1	144.4	L	3.7	
77 07 20	01 02 46	22.1	144.4	L	4.2	
77 08 28	01 41 31	22.1	144.4	L	4.5	
AU5						
67 05 29		28.8	140.5	T	MCDONALD CRISIS	
77 12/11	TO 12/18	29.07	140.23	L	MCDONALD CRISIS	
79 09/30	TO 10/01	29.07	140.23	L	MCDONALD CRISIS	
AU6						
79 11 20	06 46 04.4	26.57	138.84	R	5.3	
	GB NORTH AND EAST OF GAMBIER ISLANDS					
GB1						
75 05 14	11 49 42.3	17.43	136.05	R	5.0	
GB2						
74 03 01	02 31 27	17.0	135.1	L	3.3	
GB3						
70 03 27	22 25 25	18.1	133.7	L	3.1	
71 09 06	22 00 56	18.1	133.7	L	3.5	
GB4 ******	REGION B ******					
65 03 06	11 10 53.1	18.40	132.90	T	5.5	*B1
66 09 18	06 46 35.5	18.48	132.81	R	5.0	*B2
68 05 01	08 59 03	18.4	132.8	L	4.5	
68 08 18	05 41 28	18.4	132.8	L	4.7	
71 08 07	14 47 59	18.4	132.8	L	4.2	
72 05 13	11 24 49	18.4	132.8	L	3.3	
75 05 15	02 09 35	18.4	132.9	L	3.1	
75 05 25	14 16 32.8	18.46	132.79	R	5.0	*B3
75 09 13	18 17 41	18.4	132.9	L	3.6	
76 04 15	08 02 12	18.4	132.9	L	3.4	
77 09 22	06 02 51	18.4	132.9	L	2.7	
79 05 31	01 15 49	18.4	132.9	L	3.3	
GB5 ******	REGION C ******					
76 08 29	06 04 44	20.8	126.7	A	3.8	
76 08 30	06 50 39	20.8	126.7	A	3.1	
76 08 30	22 04 33	20.8	126.7	A	3.2	
76 08 31	03 36 36	20.8	126.7	A	3.2	
76 08 31	03 58 40	20.8	126.7	A	3.5	
76 08 31	06 19 37	20.8	126.7	A	3.5	
76 08 31	08 59 19	20.8	126.7	A	3.0	
76 08 31	09 07 14	20.8	126.7	A	3.7	
76 08 31	21 09 35	20.8	126.7	A	3.6	
76 08 31	22 40 45	20.8	126.7	A	3.2	
76 09 01	12 40 38	20.8	126.7	A	3.2	
76 09 01	15 32 42	20.8	126.7	A	3.5	
76 09 02	02 02 11	20.8	126.7	A	3.4	
76 09 05	04 57 46	20.8	126.7	A	3.4	
76 09 09	00 36 46	20.8	126.7	A	2.9	
76 09 09	21 49 35	20.8	126.7	A	3.0	
76 09 10	12 29 12	20.8	126.7	A	3.4	
76 09 10	21 15 15	20.8	126.7	A	3.7	
76 09 15	01 07 58	20.8	126.7	A	3.4	
76 09 15	20 43 53	20.8	126.7	A	3.5	
76 09 19	17 44 51	20.8	126.7	A	3.0	
76 09 23	03 19 37	20.8	126.7	A	3.7	
76 09 23	08 42 55	20.8	126.7	A	3.3	
76 09 24	06 56 18	20.8	126.7	A	3.7	
76 09 26	12 33 08	20.8	126.7	A	3.5	
76 09 28	17 38 22	20.8	126.7	A	3.2	
76 09 28	17 36 43	20.8	126.7	A	3.2	
76 09 29	04 29 17	20.8	126.7	A	3.5	
76 09 29	04 20 09	20.8	126.7	A	3.7	
76 09 29	09 37 46	20.8	126.7	A	3.4	
76 09 30	20 06 24	20.8	126.7	A	3.5	
76 10 04	07 20 58	20.8	126.7	A	3.9	
76 10 07	04 12 49	20.8	126.7	A	3.5	
76 10 08	02 52 43	20.8	126.7	A	3.4	
76 10 22	19 12 31	20.8	126.7	A	3.6	
76 10 24	06 17 20	20.8	126.7	A	3.6	
76 10 24	13 29 03	20.8	126.7	A	3.2	
76 10 26	15 23 04	20.8	126.7	A	3.2	
76 10 26	16 01 45	20.8	126.7	A	3.2	
76 10 27	05 44 08	20.8	126.7	A	3.4	
76 10 28	13 55 27	20.8	126.7	A	3.4	
76 10 29	20 32 55	20.8	126.7	A	3.8	
76 10 30	05 19 48	20.8	126.7	A	3.7	
76 10 31	04 45 15	20.8	126.7	A	3.3	
76 10 31	08 19 13.5	20.79	126.89	R	5.1	
76 11 07	17 06 59	20.8	126.7	A	3.4	
76 11 03	06 31 29	20.8	126.7	A	3.0	
76 11 04	01 42 05	20.8	126.7	A	3.0	
76 11 04	15 53 38	20.8	126.7	A	3.0	
76 11 14	20 43 18	20.8	126.7	A	3.4	
76 11 05	11 08 56	20.8	126.7	A	3.4	
76 11 09	15 06 08	20.8	126.7	A	3.4	
76 11 12	05 55 54	20.8	126.7	A	3.4	
76 11 13	23 45 16	20.8	126.7	A	3.2	
76 11 19	03 28 17	20.8	126.7	A	3.9	
76 11 29	00 51 08	20.8	126.7	A	3.8	
77 01 01	03 27 23	20.8	126.7	A	4.0	
77 01 01	22 59 08	20.8	126.7	A	4.0	
77 01 03	07 50 30	20.8	126.7	A	3.9	
77 01 05	03 23 24.9	20.89	126.93	R	5.5	*C1
77 01 31	11 03 35	20.8	126.7	A	3.6	
77 02 04	12 59 58	20.8	126.7	L	4.5	
77 04 12	19 15 27	20.8	126.7	A	4.2	
77 05 06	21 37 45	20.8	126.7	A	3.5	
77 06 19	16 54 54	20.8	126.7	A	3.4	
77 07 13	18 04 19.6	20.74	127.00	T	5.1	
77 07 25	07 54 07.5	20.80	126.94	R	5.4	*C2
77 08 27	01 58 18	20.8	126.7	A	3.6	
77 09 02	02 53 45	20.8	126.7	A	3.6	
77 09 13	12 16 38	20.8	126.7	A	3.8	
77 11 05	14 41 31	20.8	126.7	A	3.5	
77 11 06	10 29 46	20.8	126.7	A	3.8	
77 11 07	08 30 28	20.8	126.7	A	3.8	
77 11 14	07 26 39	20.8	126.7	A	3.7	
77 11 13	03 24 38	20.8	126.7	A	3.6	
77 11 13	10 04 02	20.8	126.7	A	3.9	
77 11 13	14 13 09	20.8	126.7	A	3.7	
77 11 15	04 21 41	20.8	126.7	A	3.6	
77 11 16	05 14 10	20.8	126.7	A	3.4	
77 11 16	22 15 12	20.8	126.7	A	3.4	
77 11 17	03 54 14	20.8	126.7	A	3.5	
77 11 18	18 02 19	20.8	126.7	A	3.8	
77 11 18	02 03 56.3	20.97	126.05	R	5.1	
77 11 24	12 36 57	20.8	126.7	A	3.6	
77 11 25	11 16 38	20.8	126.7	A	4.1	
77 12 02	17 35 52.9	20.75	127.26	T	4.9	
77 12 06	12 36 25	20.8	126.7	A	3.5	
77 12 16	06 58 52	20.8	126.7	A	4.1	
77 12 26	06 34 53	20.8	126.7	R	5.1	
78 04 17	09 19 21	20.8	126.7	A	3.8	
78 04 17	09 28 49	20.8	126.7	A	4.1	
78 05 19	15 32 04	20.8	126.7	A	3.7	
78 05 24	15 34 02	20.8	126.7	L	4.8	
78 06 29	18 52 14	20.8	126.7	L	4.0	
GB6						
78 01 30	18 34 19.6	16.23	136.94	R	5.0	
GB7						
78 11 06	09 05 54	22.0	132.8	L	4.5	

permanent and temporary stations in Polynesia. Residuals at the Polynesian stations were computed using the P_n propagation model of *Talandier and Bouchon* [1979], which incorporates station corrections derived from refraction surveys and an anisotropic P_n wave speed of the form

$$V(P_n) = 8.04 + 0.15\cos(2\phi + 106°) \quad (1)$$

where ϕ is the azimuth of propagation, measured clockwise

TABLE 3. Seismicity of the Tahiti-Méhétia Area, 1965–1979

DATE	ORIGIN TIME	EPICENTER	PRECIS.	DEPTH	MAG.	TYPE
Y M D	H M S	S W	KM	KM	ML	
TM : TAHITI-MEHETIA AREA						
TM1 NUMBER OF EVENTS : 15						
66 09 06	16 42 52.0	17.62 147.87	10	M	2.2	A1
66 11 21	11 55 55.0	17.62 147.87	10	M	2.7	A1
71 06 14	05 16 45.0	17.62 147.87	10	M	2.1	A1
73 04 03	08 40 7.0	17.62 147.87	10	M	1.8	A1
73 04 04	11 43 41.0	17.62 147.87	10	M	1.8	A1
78 06 11	20 24 25.0	17.88 147.60	5	M	2.6	A1
TM2 NUMBER OF EVENTS : 12						
67 07 11	13 30 2.0	17.22 148.05	6	M	2.1	A1
72 11 18	12 38 11.5	17.22 148.09	4	M	2.1	A1
72 12 01	03 55 25.5	17.29 148.04	4	M	2.6	A1
74 08 21	00 09 9.0	17.24 148.05	6	M	2.0	A1
75 02 02	18 19 59.3	17.27 148.09	4	M	2.5	A1
75 02 02	19 28 47.2	17.27 148.09	4	M	1.9	A1
TM3 NUMBER OF EVENTS : 10						
71 05 20	18 08 40.5	17.27 148.75	4	M	2.2	A1
TM4 NUMBER OF EVENTS:)400 ***** MOUA PIHAA SEAMOUNT *****						
66 03/09 TO 03/20		18.32 148.67		S		B
69 04 24	08 28 26.4	18.32 148.67	4	40	3.1	A2
69 04 29	07 08 9.3	18.32 148.67	4	40	2.8	A2,B
70 06/21 TO 06/24		18.32 148.67		S		A,B
TM5 NUMBER OF EVENTS : 10						
69 07 11	13 54 30.8	17.57 148.77	6	30	2.9	A2
75 09 10	13 08 59.1	17.57 148.77	6	30	2.5	A2
75 08 13	05 19 31.	17.57 148.77	10	30	1.8	A2
TM6 NUMBER OF EVENTS : 10						
68 01 02	11 15 14.0	17.79 148.87	6	30	2.8	A2
68 10 19	08 26 13.2	17.79 148.87	3	30	2.9	A2
TM7 NUMBER OF EVENTS : 8						
72 05 26	09 04 11.5	17.63 149.02	4	40	3.5	A2 F
72 05 26	11 40 46.3	17.63 149.02	4	40	3.5	A2 F
TM8 NUMBER OF EVENTS : 1						
65 09 25	20 29 11.0	19.12 149.17	15	M	2.7	A1
TM9 NUMBER OF EVENTS : 1						
72 01 05	13 23 42.0	18.78 149.55	6	M	3.2	A1
TM10 NUMBER OF EVENTS: 200 ***** Y.RDCARD SEAMOUNT *****						
71 09 06		17.64 148.60		S		B
72 07 08	09 28 49.0	17.64 148.60	3	MS	2.9	B
72 07 08	09 31 54.0	17.64 148.60	3	MS	2.9	B
TM11 NUMBER OF EVENTS : 15						
73 08 24	12 41 11.2	17.24 149.15	4	30	2.3	A
TM12 NUMBER OF EVENTS : 4						
73 07 19	14 49 28.7	17.56 148.97	3	30	3.1	A2
TM13 NUMBER OF EVENTS : 10						
67 07 18	10 05 16.5	17.45 149.00	4	40	2.0	A2
70 12 16	15 17 22.0	17.45 149.00	6	40	1.9	A
73 02 15	03 48 47.0	17.45 149.00	6	40	1.5	A
TM14 NUMBER OF EVENTS : 3						
71 07 20	10 30 38.0	16.40 147.92	6	M	1.8	A1
71 08 03	16 40 48.0	16.40 147.92	6	M	1.5	A1
TM 15 NUMBER OF EVENTS : 2						
70 05 17	16 27 6.0	17.28 149.01	4	M	1.7	A1
TM16 NUMBER OF EVENTS : 10						
73 11 02	11 47 3.0	18.00 149.35	10	M	1.0	A1
79 03 19	22 05 49.0	18.00 149.35	10	M	1.9	A1
TM17 NUMBER OF EVENTS : 10						
74 05 25	10 26 17.0	17.65 149.76	10	M	1.5	A1
TM18 NUMBER OF EVENTS : 500						
71 04 07	14 02 18.0	18.12 148.84	6	M	1.8	A1
75 01 20	21 21 8.5	18.12 148.84	4	M	2.6	A1
78 03 28	12 42 3.9	18.12 148.84	6	M	2.3	A1
TM19 NUMBER OF EVENTS : 1						
79 05 30	09 41 32	17.37 148.80	10	20	3.5	A1
TM20 NUMBER OF EVENTS : 12						
74 12 15	12 04 50.0	18.30 147.12	8	M	2.8	A1
74 02 24	02 45 5.0	18.30 147.12	10	M	2.2	A1
TM21 NUMBER OF EVENTS : 1						
74 11 29	11 13 58.9	16.92 149.04	6	M	2.2	A1
TM22 NUMBER OF EVENTS : 4						
75 02 08	07 24 13.2	16.82 147.56	6	M	2.3	A1
75 03 09	01 51 27.0	16.82 147.56	6	M	1.3	A1
75 11 15	03 22 37.0	16.82 147.56	6	M	2.3	A1
TM23 NUMBER OF EVENTS : 37						
75 04 24	02 15 18.4	17.83 149.51	3	25	3.2	A1
77 09 02	19 39 37.0	17.83 149.51	3	25	2.9	A1
TM24 NUMBER OF EVENTS : 11						
75 06 28	12 33 22.1	19.08 148.96	6	M	2.7	A1
77 06 30	02 19 38.0	19.08 148.96	6	M	1.9	A1
77 07 03	00 30 10.0	19.08 148.96	6	M	1.9	A1
77 07 04	02 18 32.3	19.08 148.96	6	M	3.1	A1
77 11 03	00 13 25.0	19.08 148.96	6	M	2.0	A1
TM25 NUMBER OF EVENTS : 7						
75 08 31	01 04 36.0	17.25 148.85	6	30	1.6	A1
75 10 06	21 36 43.5	17.25 148.85	3	30	2.9	A1
TM26 NUMBER OF EVENTS : 7						
75 10 29	10 41 32.4	17.72 148.89	4	30	2.9	A2
TM27 NUMBER OF EVENTS : 3						
75 03 23	02 34 5.0	16.87 149.28	6	M	2.3	A1
TM28 NUMBER OF EVENTS : 3						
77 08 12	19 33 0.3	17.32 148.95	6	30	2.9	A1
77 09 06	09 32 6.0	17.32 148.95	6	30	2.5	A1
TM29 NUMBER OF EVENTS : 3						
78 04 14	23 48 57.0	16.00 150.16	10	20	2.1	A1
78 09 23	08 46 56.0	16.00 150.16	10	20	2.7	A1
79 04 06	22 50 02.0	16.00 150.16	10	20	3.0	A1
TM30 NUMBER OF EVENTS : 2						
77 03 22	05 16 31.1	17.70 147.70	10	M	2.5	A1
77 04 13	11 52 45.1	17.70 147.70	10	M	2.4	A1
TM31 NUMBER OF EVENTS : 1						
78 10 02	02 40 15.0	17.80 149.70	10	20	1.1	A1
TM32 NUMBER OF EVENTS : 3						
79 11 04	04 42 25.9	16.35 147.37	6	30	2.3	A1
79 11 05	13 33 54.	16.35 147.37	6	30	2.0	A1
79 11 12	00 31 59.	16.35 147.37	6	30	1.8	A1
TM33 NUMBER OF EVENTS : 1						
79 10 31	03 01 33.9	19.40 149.88	10	M	2.7	A1

KEY TO EVENT TYPE (TALANDIER & KUSTER, 1976) :
A1 : ALPHA-1 TYPE
A2 : ALPHA-2 TYPE
B : BETA TYPE

KEY TO DEPTH :
M : MOHO
S : SURFACE

F : EVENT FELT ON TAHITI

from north, and the numerical values are in km/s. This velocity structure was obtained from the study of a few large well-located events and has been supported by observations of Rayleigh wave dispersion [*Okal and Talandier*, 1980*a*]. A similar procedure was used to relocate two events in Region C. The other relocations, lying outside the French Polynesian Network in Region A, were derived from teleseismic readings alone. However, the P_n residuals computed at Polynesian stations using (1) were, in all but one case, improved by relocation.

Events of magnitude less than 4.4 were below the location threshold of the global networks; hence, their epicenters were determined only by stations of the French Polynesian Network. Tentative locations were first assigned on the basis of $S_n - P_n$ times, and these were refined by an iterative procedure that minimized the residuals of the P_n arrivals. The location

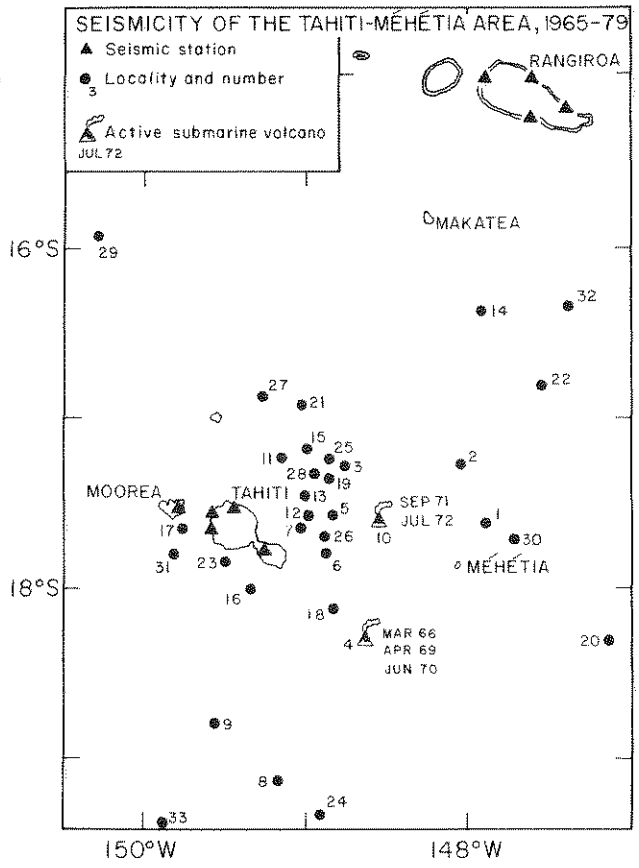

Fig. 4. Seismic localities in the Tahiti-Méhétia area. Numbers correspond to epicenter designations in Table 3; active submarine volcanoes Moua Pihaa (4) and Yves Rocard (10) and dates of recorded volcanic crises are indicated. Figure updates Figure 5 of *Talandier and Kuster* [1976].

algorithm employed *Talandier and Bouchon*'s [1979] P_n propagation model, given by (1). Epicenters obtained in this manner are labelled *L*, for local, in Table 2. The location accuracy is a function of the epicentral position relative to the array and the number of readings available; except for a few earlier events predating implementation of the full network and those events far removed from the array, the precision is on the order of 20 km.

Earthquakes of sufficiently low magnitude are occasionally recorded at a single station, thus providing only an estimate of the epicentral distance from the $S_n - P_n$ differential travel time. In such cases tentative locations have been assigned when the events share waveform and spectral characteristics with other well-located events of larger magnitude. Locations of this type are labelled *A*, for approximate, in Table 2, and they correspond to swarm events in cluster GB5 (Region C).

Given the poor depth resolution available for the earthquakes in Table 2, no hypocentral depths are listed. Observations of surface-reflected phases, discussed below, imply that the larger events are probably confined above the crust-mantle interface, however.

Table 3 lists the locations of events in the Tahiti-Méhétia area, where the relatively dense station coverage permits some resolution of hypocentral depth for events occurring beneath the Mohorovičić discontinuity. The location techniques of *Talandier and Kuster* [1976] were used, which employ crustal models derived from refraction experiments in the area: the model for Tahiti features a 17-km crustal thickness and a P_n velocity of 8.3 km/s; the model for Rangiroa has a 26-km crustal thickness and a P_n velocity of 7.9 km/s.

The estimates of local magnitude listed in Tables 2 and 3 were computed from a relation similar to *Richter*'s [1935]:

$$M_L = \log(A/T) + B \log \Delta + C \qquad (2)$$

Here A is the peak-to-peak amplitude in microns at a period T near 1 s, and Δ is the epicentral distance in kilometers. The coefficient B was empirically determined from P_n amplitude decay with distance to be 2.5. The parameter C is a station-dependent constant that ensures continuity at large magnitudes with the teleseismically determined m_b values; its values range from −2.1 (Tahiti, Rangiroa, Hao) to −1.5 (Tubuai) to −1.3 (Rikitéa). Magnitudes determined from this parameterization typically show fluctuations across the network of about 0.3 units. Much of the variation can be ascribed to P_n propagation anomalies observed in French Polynesia, notably in the area between Tahiti and Rangiroa [*Talandier and Bouchon*, 1979].

One measure of seismic activity in a given region is the total energy released by earthquakes during a particular period. For individual events the seismic energy E_s, in ergs, is estimated by *Gutenberg and Richter*'s [1954] formula,

$$\log E_s = 9.9 + 1.9 M_L - 0.025 M_L^2 \qquad (3)$$

This estimate is useful for comparisons between regions, but we do not attach significance to the absolute values.

The general features of the seismic activity are summarized in Figures 3 and 4. Although seismicity is distributed throughout the study area and includes a number of isolated events, the most prominent feature of the activity outside the Tahiti-Méhétia area is the distinct clustering of events at approximately 13 localities. A comparison of the event locations in Table 2 and Figure 3 reveals that the epicentral separations within a cluster (typically < 50 km) are generally much less than the distances between clusters (typically > 100 km). In fact, we have found that at least some of the clusters are confined to regions whose characteristic lateral dimensions may be on the order of only 10 km.

Each cluster or isolated event has been assigned to one of six geographical zones: Line Islands (LI), Tuamotu Islands (TU), north of Society Islands (SC), Cook Islands and north of Austral Islands (NA), Austral Islands (AU), north and east of Gambier Islands (GB), and Tahiti-Méhétia (TM). The zones are outlined on Figure 2.

Three of the event clusters, LI2, GB4 and GB5, are the sites of very intense seismic activity and together account for more than 90% of the seismic energy released in the study area. These three clusters have been designated Regions A, B and C, respectively, and they are discussed in more detail in the next section.

Line Islands (LI). A total of 92 events have been recorded in this geographic zone with a cumulative energy release of 4.7×10^{19} ergs. The seismic activity is confined to three distinct localities. LI0 and LI1 are the sites of two isolated events of magnitude 4.6 and 5.2, respectively. The former occurred on January 25, 1962, just outside the study area and prior to the installation of the French Polynesian Network, and the latter on April 13, 1967. The seismicity at LI2, which we have designated Region A, was first detected in June 1968, beginning a two-year period of swarm activity. The swarms typically

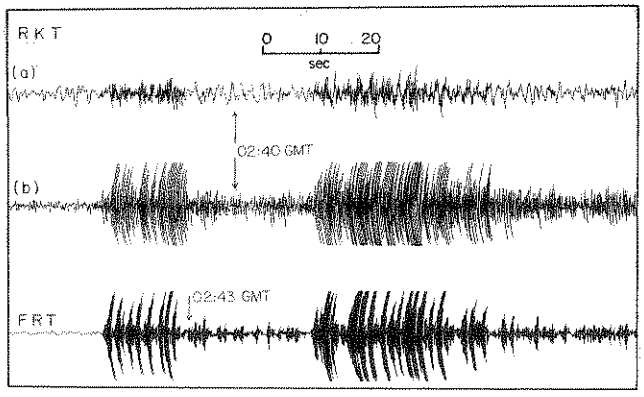

Fig. 5. Distinct *T* phase arrivals at stations RKT and FRT from initial activity of the 12/77 Macdonald crisis. Traces (*a*) and (*b*) from short-period vertical instruments at RKT with peak magnifications of 125,000 at 1 Hz and 2,000,000 at 3 Hz, respectively. FRT trace is from a short-period vertical instrument with magnification of 31,000 at 1 Hz. Sharp first arrivals allow the precise location of individual events.

lasted a few days and were separated by apparently quiescent periods of one to four weeks. Following this intense activity was a three-year hiatus, during which only a single small (M_L = 3.8) event was recorded. In January 1973 a large swarm occurred, including four events big enough (m_b = 4.4–4.9) to be located by the global networks. The termination of this swarm marked the beginning of another quiescent period lasting 17 months, after which activity was sporadic until a swarm of seven events in October 1976, when all recorded seismicity ceased.

Tuamotu Islands (TU). During the recording period of 1965–1976 the seismicity in the vicinity of the Tuamotu Archipelago was less intense than in the LI zone, with no events larger than M_L = 4.2 and with a total seismic energy release of only 5×10^{17} ergs. The low level of activity is undoubtably real, since two four-station permanent arrays in Rangiroa and Hao provide relatively good detection capabilities. Earthquakes have been located in nine separate sites (TU1–TU9) concentrated in the western and northern parts of this zone. No seismicity has been recorded from the southeastern half of the island chain.

All of the TU localities, except for TU8, are the sites of single events in the magnitude range 2.0–4.2. Fifteen events have been recorded from TU8, 12 during a five-week burst in September–November 1976 and 3 during the following six months. Except for TU9, the seismicity is roughly aligned along the tectonic axis of the archipelago, striking N65°W, and, excluding the events at TU2 and TU3, this activity shows an apparent spatial and temporal progression to the southeast, beginning in early 1966 and continuing over an eleven-year period. The isolated event at TU9 lies to the northeast of the island chain and is aligned with localities in the GB area.

Northwest of Society Islands (SC). The seismic characteristics of the two proximate localities SC1 and SC2 differ somewhat from those of the TU group to the north and east. Earthquakes at SC1 and SC2 are low in magnitude ($M_L \leq 3.6$, total energy release $\sim 4 \times 10^{16}$ ergs), but, unlike the activity at LI2 and TU8, the seismicity is not clustered in swarms. In fact, all but two of the 15 events are separated by quiescent intervals of four weeks or longer, and the median recurrence time for the period 1969–1978 is over six months. According to the bathymetric map of *Mammerickx et al.* [1975], the two epicenters lie near an elongated seamount with a SE-trending major axis about 50 km in length that rises approximately 800 m above the ocean floor. In the absence of more detailed bathymetric and seismic surveys, however, the significance of this relationship is not known. On November 14, 1979, a single event was recorded at a new locality, SC3, under the island of Raiatea, in the Leeward group of the Society Islands. This isolated earthquake had a local magnitude of 2.4.

Cook Islands and north of Austral Islands (NA). The four localities situated within this zone had a cumulative seismic energy release of 1.4×10^{17} ergs during the recording period. Both NA1 and NA3 are the sites of single events, although NA1 is sufficiently far removed from the network to preclude the detection of events below M_L = 3.5, and lower level seismicity could therefore be missed. Four events occurred at NA2 from 1968 to 1975 separated in time by six months to five years. NA4 is the most active locality in this zone, with 24 events detected between mid-1974 and the end of 1979.

Austral Islands (AU). Substantial seismicity has been recorded in the vicinity of the Austral Islands, with M_L values

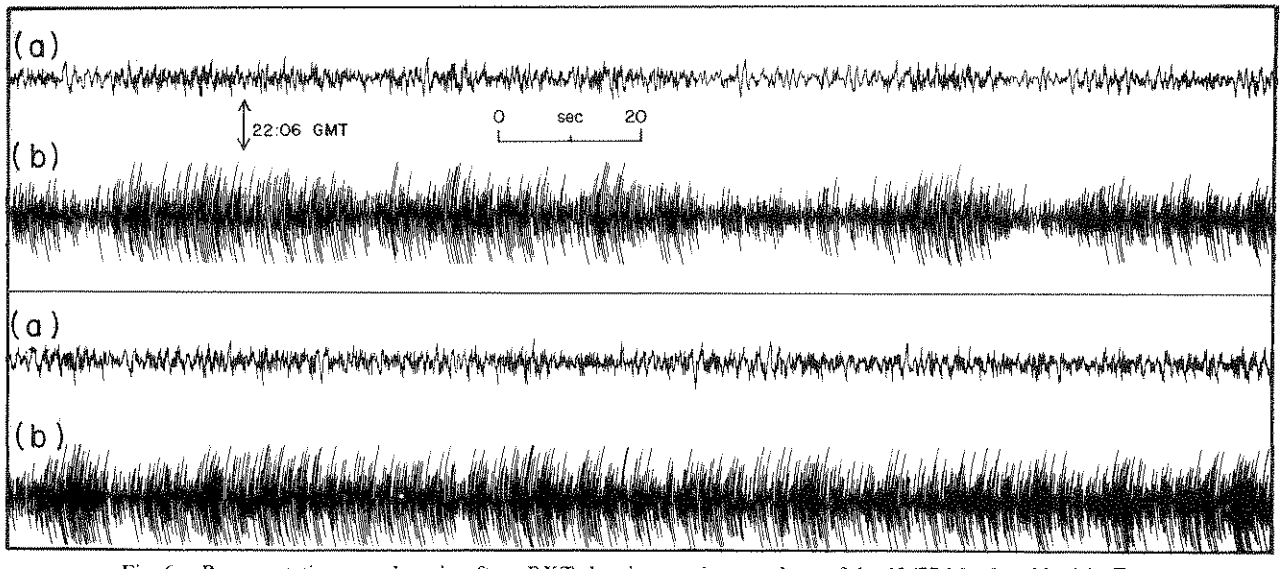

Fig. 6. Representative record section from RKT showing continuous phase of the 12/77 Macdonald crisis. Traces (*a*) and (*b*) are the same as in Figure 5; second pair of traces is the continuation of the first. The noise activity continues for about 1 week.

TABLE 4. Major Events ($m_b \geq 4.9$) Recorded in the South Central Pacific During 1965–1979

Locality	Date	Origin Time, UT	Latitude, °S	Longitude, °W	m_b	Event Identification
LI1	April 13, 1967	1426:49.5	7.0	151.0	5.2	
LI2	July 29, 1968	0245:44.5	7.5	148.3	4.9	A_1
(Region A)	Aug. 6, 1969	1715:39.7	7.4	148.4	5.1	A_2
	Jan. 19, 1973	0736:32.9	7.4	148.3	4.9	A_3
	Jan. 19, 1973	1526:26.1	7.3	148.3	4.9	A_4
AU6	Nov. 20, 1979	0645:02.8	26.8	138.9	5.3	
GB1	May 14, 1975	1149:41.9	17.6	136.3	5.0	
GB4	March 6, 1965	1110:53.1	18.4	132.9	5.5	B_1
(Region B)	Sept. 18, 1966	0640:37.8	18.4	132.8	5.0	B_2
	May 25, 1975	1416:33.7	18.4	132.8	5.0	B_3
GB5	Oct. 31, 1977	0819:14.5	20.8	126.7	5.1	
(Region C)	Jan. 5, 1978	0323:27.9	20.8	126.9	5.5	C_1
	July 13, 1978	1804:19.6	20.7	127.0	5.1	
	July 25, 1978	0754:09.0	20.7	126.9	5.4	C_2
	Oct. 18, 1978	0203:59.0	20.8	126.7	5.1	
	Feb. 26, 1979	0631:53.0	20.8	126.7	5.1	
GB6	Jan. 30, 1978	1834:21.0	16.2	126.3	5.0	

up to 5.3 and with a total seismic energy release for the period 1965–1979 exceeding 2.4×10^{19} ergs. We have identified six active localities. AU3, the site of a single $M_L = 4.0$ earthquake in January 1972, is located along a locally well-defined portion of the Austral Fracture Zone, a feature belonging to the ENE-trending system of fractures formed by the Pacific-Farallon ridge [*Herron*, 1972]. On the other hand, the three localities AU1, AU2, and AU4 do not appear to be associated with any prominent bathymetric feature.

Four events in the magnitude range 3.5–4.4 were recorded from AU1 during a seven-month period in 1970, and three of comparable magnitude (3.7–4.5) were located at AU4 during 1977. AU2 was the site of a single event in 1970 ($M_L = 4.5$) but otherwise remained quiescent until April, 1977, when a series of 23 events was initiated. The series terminated with a swarm of 7 locatable events in June 1978 and was followed by an isolated event in May, 1979.

Locality AU5 is the site of Macdonald Volcano, situated at 28.98°S and 140.24°W [*Johnson and Malahoff*, 1971]. During the interval 1965–1979 there have been three known episodes of seismicity. The first occurred on May 29, 1967, generating for a period of about five hours *T* waves which were recorded in Hawaii and which led to the initial discovery of Macdonald [*Johnson*, 1970]. At this time, neither stations TBI and VAH nor the Hao array existed, and the stations favorably located for the reception of *T* waves from Macdonald, PAE and RKT, were not equipped for high-gain, high-frequency operation. Hence, the 1967 event was not recorded in French Polynesia.

Between December 11 and 18, 1977, *T* phases generated by a second crisis at Macdonald were recorded all over Polynesia. Strong individual events at the beginning of the crisis gave rise to sharp arrivals at various stations in the network (Figure 5). The location computed from these arrivals (29.07°S, 140.23°W) is only 10 km from the crest of the seamount. Almost continuous activity was recorded until 0130 GMT on December 15, with subsequent sporadic noise activity lasting until December 18. A typical record from the continuous phase of the crisis is displayed in Figure 6. The crisis was recorded at stations PAE, VAH, FRT, RKT, and TBI and, in fact, was clearly evident on channels set at the low gains available in 1967. Since the 1967 crisis was not recorded, we conclude that the 1977 activity was more intense.

Recently, between September 30 and October 1, 1979, another Macdonald crisis was detected from *T* phase activity in Polynesia. The crisis began suddenly at 12:46 GMT on September 30. The continuous generation of seismic noise, similar in character to the previous crisis (Figure 6), apparently ceased only two days after its initiation. By this measure the 1979 crisis was thus less intense than the 1977 crisis.

A new bathymetric survey of Macdonald seamount may be warranted to check whether or not the two recent crises have been associated with significant surficial vulcanism.

Finally, on November 20, 1979, a strong earthquake was registered from a new locality (AU6) approximately 250 km northeast of Macdonald seamount. A tentative magnitude of $m_b = 5.3 \pm 0.2$ was obtained from 10 WWSSN records, making this the largest isolated event in our study area (only earthquakes in Regions B and C have been stronger). The epicenter is not associated with any known bathymetric feature.

North and east of the Gambier Islands (GB). The greatest concentration of seismic activity in French Polynesia has occurred within a zone to the north and east of the Gambier Islands, comprising 7 localities with a cumulative 1965–1979 energy release of 1.9×10^{20} ergs. The seismic centers GB1–GB4, together with TU9, are aligned along an axis oriented approximately N64°W, which coincides with the northeastern margin of the Tuamotu Island platform [*Mammerickx et al.*, 1975]. GB5 lies near an extension of this axis to the southeast, but neither it nor GB6 and GB7 are associated with any major bathymetric features. The ship-track coverage in this area is extremely poor, however.

Only GB4 and GB5 are the loci of more than two events, and we have designated these localities Region B and Region C, respectively. Teleseismically located events with body-wave magnitudes up to 5.5, the largest in Polynesia, have been recorded within both clusters. Region B seismicity consists of 12 events more-or-less uniformly distributed over the fifteen-year recording interval. In contrast, Region C was quiescent until the initiation in August 1976 of intense seismic activity. Except for a one-year gap (October 1976 to October 1977) this activity was fairly continuous through June, 1979. Thus far, 96 events have been located in Region C.

Tahiti-Méhétia (TM). The seismicity of the Tahiti-Méhétia area prior to 1975 has been described in detail by *Talandier and Kuster* [1976], so the present discussion serves mainly to update their report. Thirty-three active localities can be resolved. Table 3 and Figure 4 display the epicentral

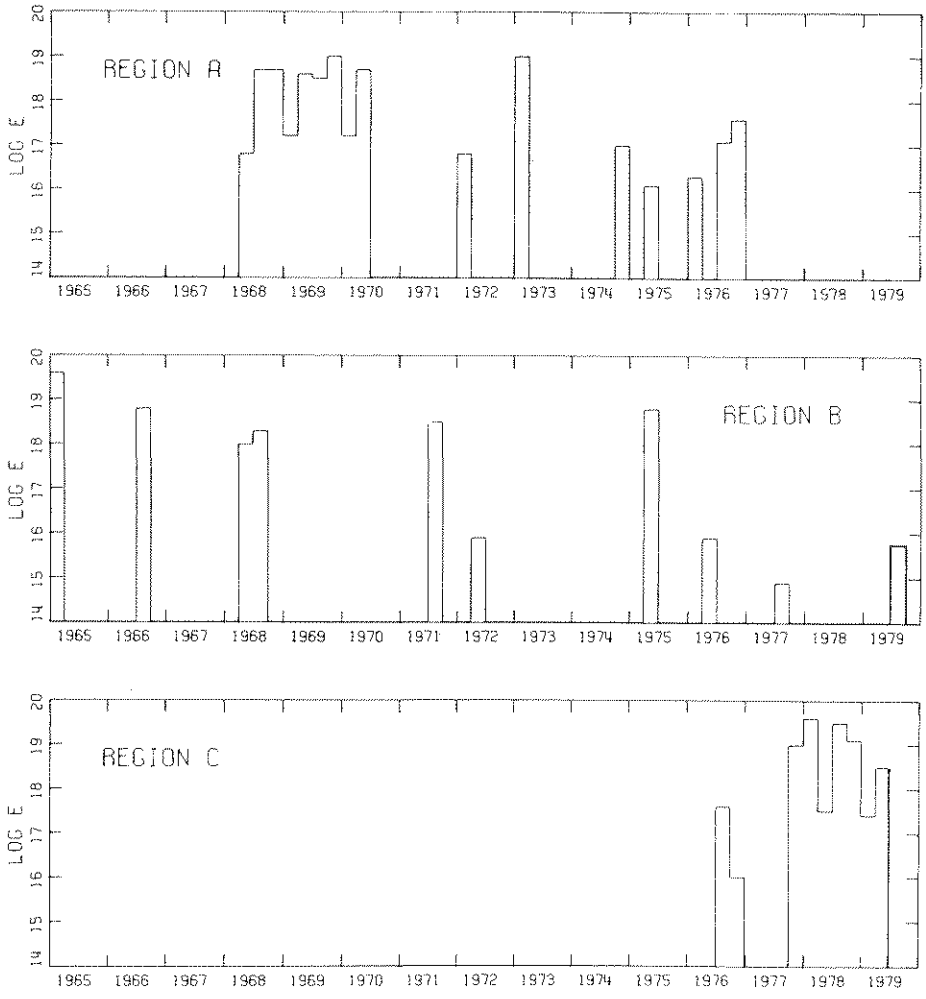

Fig. 7. Histograms of seismic energy release in Regions A, B, and C for the period 1965–1979. Class intervals are quarters. Detection thresholds for individual events are approximately 3×10^{14} ergs, except in Region C, where the detection threshold prior to 1967 is $\sim 10^{18}$ ergs.

information for the earthquakes with $M_L \geq 1.3$ occurring between 1965 and 1979. In addition, Table 3 gives rough estimates of hypocentral depth, as well as the total number of events associated with each locality.

Over the period 1975 to 1979, four of the localities listed by *Talandier and Kuster* [1976] were re-activated, including TM5, which was the site of a single previous event in 1969. Locality TM18 continued to be active at the rate of 30 to 50 events a year, most notably in 1975 and 1978. A total of 15 new localities were identified. Most earthquakes during this period were shallow events of the α_1 type [*Talandier and Kuster*, 1976], although occasional deeper, high-frequency events (α_2 type) were recorded. Since 1975 no β type activity, characterized by shallow swarms with low-frequency spectra, has been detected. *Talandier and Kuster* [1976] have hypothesized that β type events are diagnostic of submarine vulcanism. If so, the two volcanoes at TM4 and TM10 (Moua Pihaa and Y. Rocard seamounts) have remained magmatically quiescent during 1975–1979.

No earthquakes originating in Polynesia were felt over this period (two events from TM7 were felt in 1972). The tremors felt on June 22, 1977, by residents of Tahiti were due to *T* waves propagated from a Tonga event [*Talandier and Okal*, 1979].

DETAILED SEISMIC STUDIES OF REGIONS A, B, AND C

Earthquakes in the South Central Pacific with body-wave magnitudes greater than or equal to 4.9 are summarized in Table 4. Only three localities, LI2, GB4 and GB5, have been the sites of more than one such event; following our previous usage [*Jordan et al.*, 1978; *Sverdrup and Jordan*, 1979], they are designated Regions A, B and C, respectively. To gain a better understanding of the relationships between the seismicity in these regions and intraplate tectonics of the South Central Pacific, we have investigated their properties in more detail. Focal mechanisms for 8 of the larger earthquakes have been determined, and constraints on their hypocentral depths have been established. In addition, *Sverdrup and Jordan* [1979] have recently completed a detailed bathymetric survey of Region A.

Seismicity. After Hawaii, Regions A, B and C have been the most seismically active localities in the interior of the Pacific plate. One remarkable feature of this seismicity, shared by other earthquake clusters in Polynesia, is its spatial concentration. Based on the distribution of teleseismically located events (Table 2), the characteristic horizontal dimensions of the clusters in Regions A, B and C are 50 km or less. In fact, the actual sizes of the clusters could be appreciably smaller

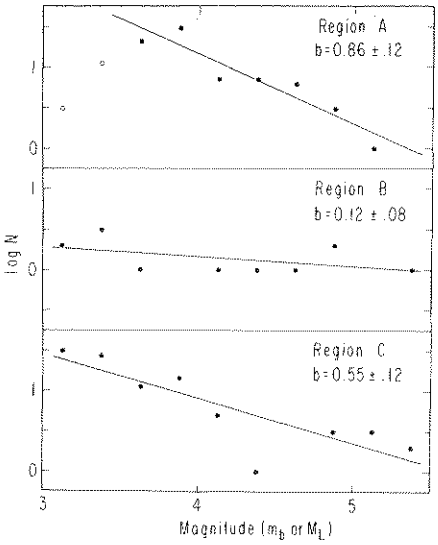

Fig. 8. Frequency-magnitude plots for Regions A, B, and C for the period 1965–1979. The b values are slopes of lines determined by regression fit to solid circles; uncertainties are one standard deviation.

than 50 km. Since the epicenters were individually determined from different station sets, the location errors are only weakly correlated, and they contribute significantly to the dispersion. To refine the bound on the cluster dimension for Region A we have computed the relative locations of events A_1–A_4 using a new joint inversion technique [*Jordan and Sverdrup,* 1980]. All four epicenters fall within a circle of radius less than 10 km. Thus, the size of this particular cluster is probably not more than one order of magnitude greater than the fault dimensions of the largest individual earthquakes occurring within it (~3 km).

A second striking feature of the seismicity in Regions A, B and C is its temporal distribution. As noted in our discussion of the event catalogue (Table 2), both regions A and C are characterized by earthquake swarms with apparent durations of one day to several weeks, whereas the activity in Region B consists of discrete events isolated in time. The contrast is also evident when the energy release is averaged over longer time scales, as illustrated by the histograms of Figure 7. During the recording period 1965–1979, the temporal distribution of earthquakes in Region B has been essentially random (Poissonian). The events in Regions A and C, on the other hand, have been much more clustered in time. The observed seismicity at each of these two localities has been confined to a single sub-interval of the recording period, or to what might be termed a 'super-swarm': June 1968 to October 1976 in the case of Region A and August 1976 to June 1979 in the case of Region C. Whether the temporal patterns suggested by Figure 7 are features of the long-term seismicity or simply artifacts of small-sample statistics is, of course, a question requiring seismic monitoring over a more extended period. The continued operation of the French Polynesian Network will be critical in this regard.

The distribution of seismicity with magnitude is documented in Figure 8. In constructing this figure event frequencies were integrated over windows of 0.25 magnitude units and the parameters of a Gutenberg-Richter exponential decay relation were determined by standard linear regression. For Region A, only events above magnitude 3.5 were used, because the points for the lower magnitude intervals show a rolloff that is probably attributable to incomplete sampling of the seismicity. The decay constants (b values) estimated for Regions A, B and C are 0.86 ±0.12, 0.12 ±0.08 and 0.55 ±0.12, respectively.

The b value for Region A is comparable to the global average, estimated to be 0.9 by *Gutenberg and Richter* [1954] and 0.78 by *Sakuma and Nagata* [1957], but those for Regions B and C are significantly less. Particularly striking is the extremely low b value for Region B. Although the sample size is small and the uncertainty in this b value is probably underestimated by the formal standard error, the anomalous distribution of magnitudes is nevertheless clear; e.g., as many events have been recorded above magnitude 4 as below. Given the proximity of Region B to station RKT (~600 km), it is unlikely that its b value is very much affected by the network sampling bias.

The higher b values in Regions A and C are consistent with the swarmlike characteristics of the seismicity in these two clusters, but they are lower than those observed for mid-Atlantic Ridge swarms (b = 1.3 [*Sykes,* 1970]), swarms in the Tahiti-Méhétia area associated with cataclastic volcanic activity (b = 1.3–3.2 [*Talandier and Kuster,* 1976]), or long-term Hawaiian seismicity (b = 1.05 ±0.14 [*Furumoto et al.,* 1973]). Care must be taken in basing inferences on these simple statistics, however. A much larger b value ($b \simeq 1.1$) is obtained for Region C if the analysis is restricted to events with $M_L < 4.75$, for example. Furthermore, we cannot discount the possibility of magnitude bias due to the saturation of P_n amplitudes.

Focal depths. Hypocentral depths of 33 km were assigned by both the USGS and ISC to all teleseismically located events in Regions A and C. In the case of the July 29, 1968, earthquake (event A_1, Table 3), however, the ISC notes that the unconstrained depth from P times is 'exceedingly negative,' suggesting a shallower value. For event B_1, the bulletin depths are 35 km (USGS), 31 ±21 km (ISC), and 21 ±1 km (ISC, $pP-P$ data); for event B_2, 42 km (USGS), 67 ±17 km (ISC) and 40 ±7 km (ISC, $pP-P$ data); and for event B_3, 19 km (USGS, $pP-P$ data) and 13 km (ISC, $pP-P$ data). As noted previously, the location procedures used by the various agencies preclude the accurate determination of focal depth in the oceanic environment.

In particular, the presence of an overlying, low-velocity water layer must be accounted for in the interpretation of $pP-P$ times. The existence of such a layer is actually advantageous, because strong multiple reflections within the water column are commonly observed, providing additional constraints on the depth of focus [*Mendiguren,* 1971; *Duschenes and Solomon,* 1977]. Following previous usage, we denote the compressional depth phase reflected n times from the sea surface by *pnwP*. Our analysis of certain secondary arrivals from events in Regions A, B and C indicates that they are *pnwP* phases from very shallow sources. Examples are illustrated in Figure 9.

The times of all prominent secondary arrivals relative to the P-wave break time for events A_1–A_4 are plotted as a function of epicentral distance in Figure 10. Superimposed are lines corresponding to the theoretical travel time differences for *pnwP* phases generated at various depths below the sediment-water interface. The oceanic crustal velocity structure assumed by the calculation was the central Pacific model of *Orcutt and Dorman* [1977], adjusted for water depth and sediment thickness using the sounding data of *Sverdrup and Jordan* [1979]. The two-way travel times through the water

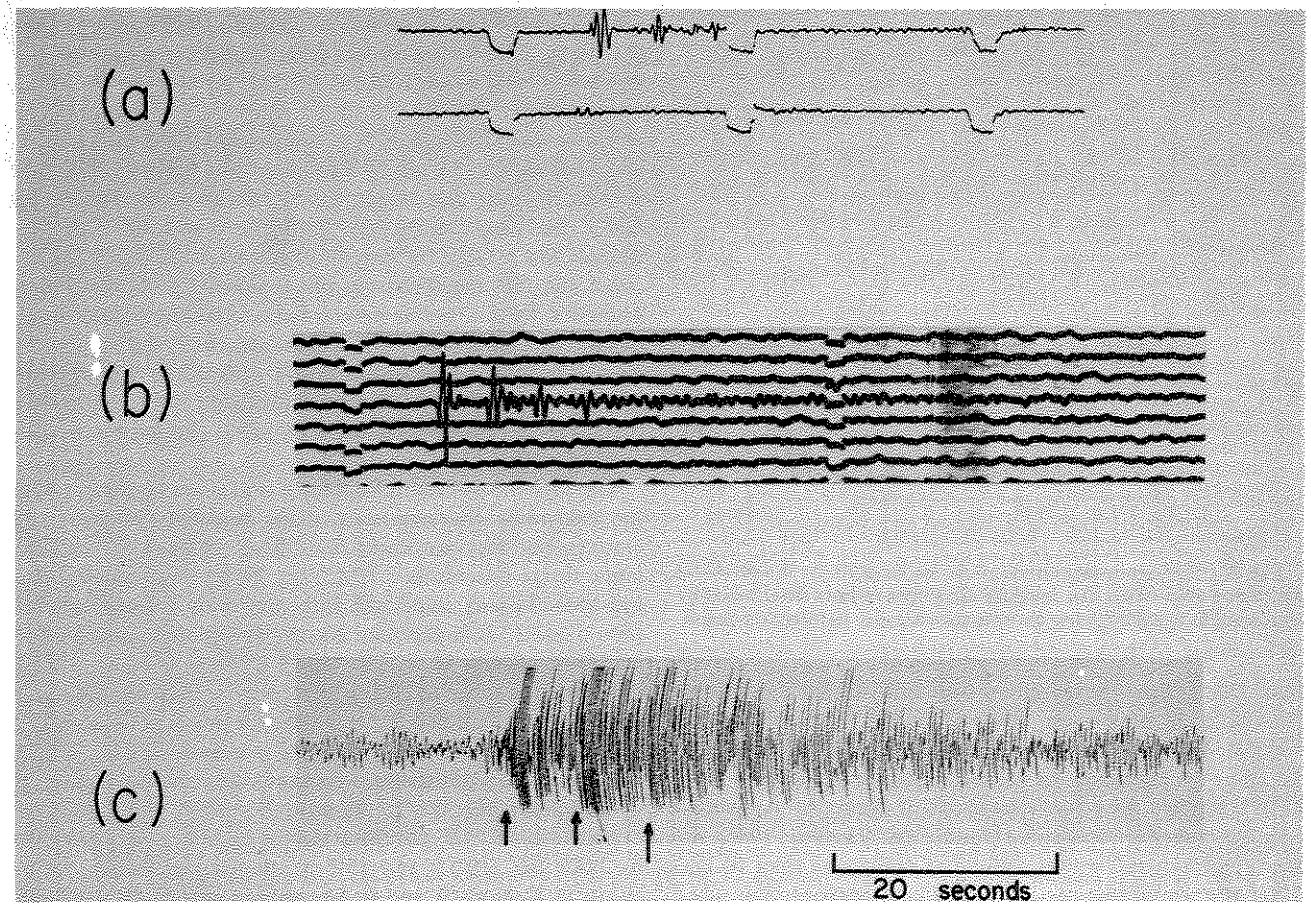

Fig. 9. Seismograms from events in Regions A, B and C showing water multiples. Trace (*a*) is vertical-component record from station WRA (Warramunga, Australia) for event A_4; time marks are at 30-s intervals, upward ground motion is down on the record. Arrivals following *P* by about 7 s and 14 s are identified as *pwP* and *pwwP*, respectively. Trace (*b*) is SPZ record from WWSSN station SNA (Sanae, Antarctica) for event B_2; time marks are at 60-s intervals, upward ground motion is up on the record. Arrivals following *P* at ~6-s intervals are identified as *pwP*, *pwwP*, and *p3wP*. Trace (*c*) is vertical-component record from station RKT (Rikitea, French Polynesia) for an event on October 31, 1977, in Region C; time scale as shown. P_n arrival and two possible water multiples are indicated by arrows.

and sediment columns above the Region A hypocenters were measured by Sverdrup and Jordan to be 7.00 s and 0.05 s, respectively, corresponding to a water depth of 5250 (uncorrected) meters and a sediment thickness of about 50 m. Most of the observed secondary arrival times in Figure 10 are consistent with the *pnwP* times predicted for sources at focal depths less than 5 km below the sediment-water interface.

Records for Region B earthquakes commonly display multiples at intervals of 6 ±1 s. A good example is provided by the short-period vertical (SPZ) seismogram of event B_2 from Sanae, Antarctica ($\Delta = 85°$); three secondary arrivals with successively smaller amplitudes can be clearly identified (Figure 9). We again interpret these arrivals to be *pnwP* phases. The repeat time between the multiples is consistent with the water depth (~4200 m) and is not significantly less than the time difference between the first and second arrivals. Based on this interpretation, a focus within a few kilometers of the sea bottom is required. An alternate but less plausible explanation would be to identify the second arrival as *pP*, the third as a combination of *sP* and *pwP*, and the fourth as *pwwP*, implying a focal depth of ~19 km below the sea floor. The shallower hypocenter is favored by the regularity of the amplitude decay and by the observations of strong *T* waves at station RKT and at a temporary station on Turéia. Two multiples following *P* by 6 s and 12 s are also apparent on a number of WWSSN records of events B_1 and B_3.

Depth phases for events in Region C are observed less often. SPZ records of event C_1 show strong secondary arrivals about 7 s after *P* at the WWSSN stations ATL and BOG, although higher multiples ($n \geq 2$) are not obviously present. A phase following the first arrival by 7 s is also seen on the high-frequency P_n records of this event at RKT. Identifying these arrivals as *pwP* and taking the water depth to be 4000 m [*Mammerickx et al.*, 1975], we calculate the hypocentral depth to be about 5 km below the sediment-water interface. Other events in Region C appear to be even shallower. Three arrivals separated by 6 ±1 s were recorded at RKT for the October 31, 1977, earthquake (Figure 9). A second arrival with the same delay is regularly observed at RKT for events of smaller magnitude and at WWSSN stations for the larger ones (e.g., event C_2). For all major events in Region C, substantial *T* waves are present at RKT. Furthermore, long trains of high-frequency (~1 Hz) waves, some lasting 20 minutes, are consistently seen at RKT. Their dispersion is evidently controlled by the soft sedimentary layer, and shallow sources are probably required for their generation [*Okal and Talandier*, 1980*b*].

In summary, the data suggest that the larger earthquakes in

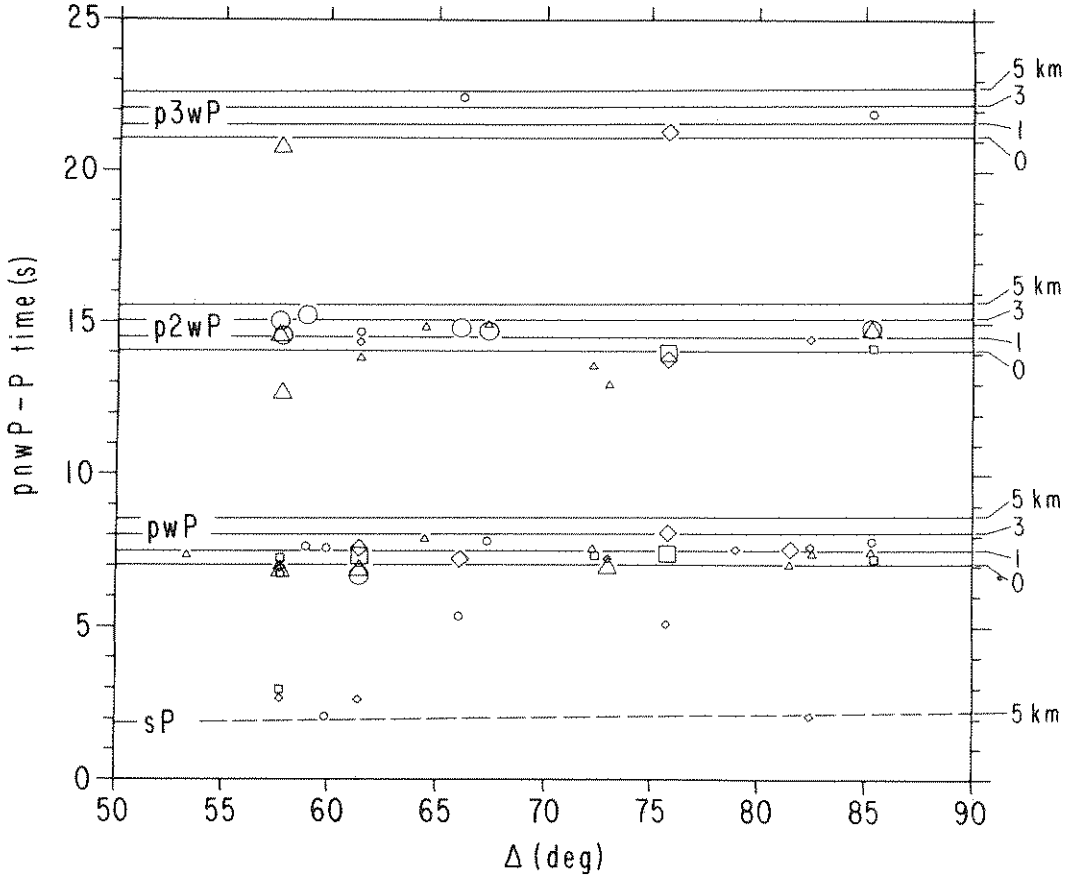

Fig. 10. Plot of *pnwP-P* differential travel times (solid lines) and *sP-P* times (dashed line) as functions of epicentral distance for various water depths, computed for a velocity model appropriate to Region A (see text). Symbols represent the times of prominent secondary arrivals relative to the *P* wave break time for events A_1 (triangles), A_2 (circles), A_3 (diamonds), and A_4 (squares); large symbols indicate impulsive arrivals, small symbols indicate emergent arrivals.

Regions A, B, and C occur within 5 km of the sediment-water interface; that is, the bulk of the seismicity is confined to the oceanic crust.

Focal mechanisms. The first-motion diagrams for 9 earthquakes are presented in Figure 11. Compared to events typically used in focal mechanism studies, these earthquakes are small ($4.9 \leq m_b \leq 5.5$); clear *P*-wave first motions were observed only on short-period records with magnifications of 25,000 or more. Because the characteristic source dimensions are small, however, the short-period waveforms are generally simple at teleseismic distances (Figure 9), and, unlike those often recorded from larger, more complex events, their first motions appear to be consistent with a point-source approximation.

Our principal data source was the WWSSN, although a number of records from other installations were also used. All readings were made by one or more of the authors. We did not use P_n arrivals from Polynesian stations, because the first motions from stations at nearly identical azimuths are often inconsistent, probably due to the complex mode of P_n propagation. *PKP* readings were used only for records where the DF branch could be clearly identified, and both *P* and *PKP* readings with residuals of more than a few seconds were discarded. Emergent arrivals were characterized as having nodal character only if recorded at sites with magnifications of 50,000 or more. Although surface-wave amplitudes at circum-Pacific stations were examined in several cases for consistency with the first-motion solutions, this information was not used directly, since these events have low surface-wave magnitudes ($3.7 \leq M_s \leq 4.5$) and did not excite the long-period (>30 s) waves necessary to avoid a strong dependence on focal depth and lateral heterogeneity in crustal structure. In computing the first-motion solutions, a *P*-wave velocity of 6.5 km/s at the hypocenter was used, consistent with our conclusion that the events occurred within the oceanic crust.

The four events from Region A have similar strike-slip mechanisms. With the exception of one nodal plane for event A_4, the solutions are reasonably well constrained. Some of the observed polarities are inconsistent with the derived mechanisms, but these generally occur at stations where the signal-to-noise ratio is low or the waveforms are anomalously complex. For example, despite the inconsistencies among the North American stations in the case of event A_1, there exists a distinct change in polarity across a subset of stations with high signal-to-noise ratio that defines the nodal plane. Our results for A_1 differ from those of *Sykes and Sbar* [1973, 1974], who classified it as a thrust in their studies of intraplate mechanisms. A significant component of thrust faulting is clearly excluded by good dilatations at stations in the southern United States, South America, Africa and Australia. For event A_4, only the EW-trending plane is well determined; the other was chosen to have a steep dip to make it consistent with event A_3, which occurred on the same day.

The three events from Region B also yield focal mechanisms with two steeply dipping nodal planes, but they are not as well constrained as those from Region A. Most of the arriv-

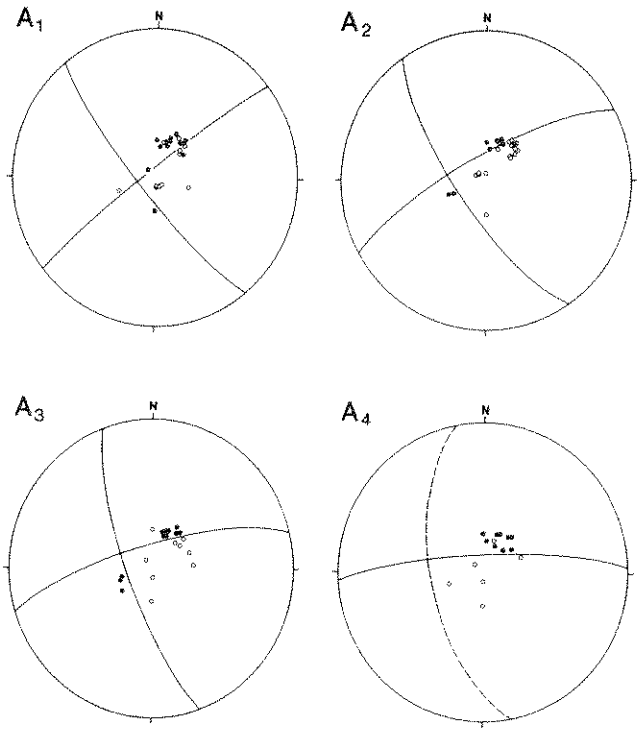

Fig. 11*a*. First-motion diagrams for four events in Region A. Solid circles are compressions; open circles are dilatations; crosses are nodal arrivals. Focal mechanism parameters are listed in Table 5; nodal plane is dashed when poorly constrained. Stereographic projection.

als from B_1 are dilatational; only the WWSSN stations CMC, ARE and LPS yield compressions. The compression at CMC is suspect, since it is surrounded by dilatations. The existence of a nodal plane separating the other two compressions from a dilatational field is corroborated by nodal arrivals at three

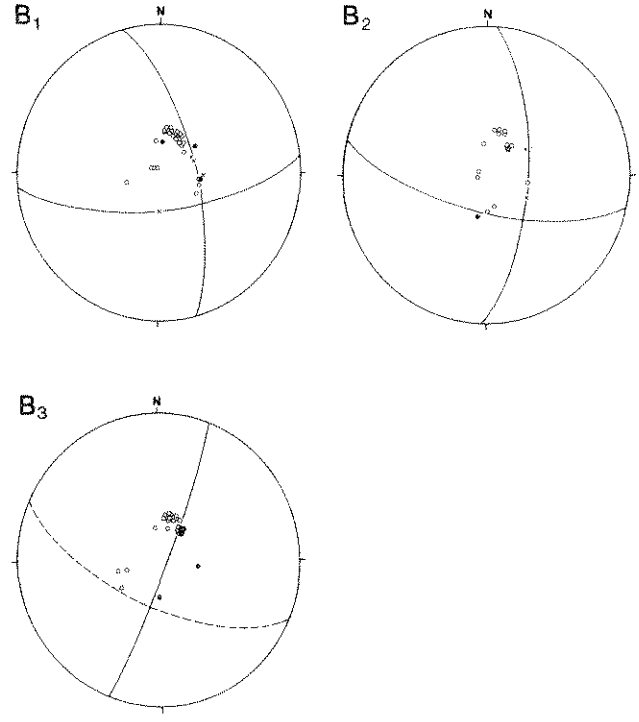

Fig. 11*b*. First-motion diagrams for three events in Region B. Conventions same as in Figure 11*a*.

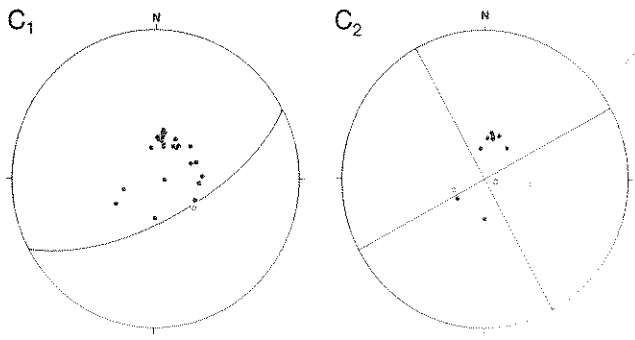

Fig. 11*c*. First-motion diagrams for two events in Region C. Conventions same as in Figure 11*a*.

high-gain (50,000) South and Central American stations. The second nodal plane was fixed by a single nodal-type arrival at the South Pole station (SPA), which operates at a gain of 100,000. Event B_2 is similar, but in this case the EW-trending nodal plane is pinned by a clear compressional arrival at SBA, whereas the other plane is fixed only by nodal arrivals at stations LPS and PEL. A single steeply-dipping nodal plane separates the compressional and dilatational fields for event B_3; the second plane was fixed by requiring similarity with the other two fault-plane solutions. Although a purely dip-slip mechanism for B_3 would satisfy the teleseismic first-motion data, a steeper dip on the second plane is more compatible with the observation of Rayleigh and Love waves of similar amplitude at PPT.

Unlike those from Regions A and B, the mechanism for event C_1 is clearly characterized by a component of thrusting; all arrivals but one were compressional. The single dilatation was recorded at a station in Valdivia, Chile. In order to satisfy this constraint, one nodal plane must have a strike between the azimuths of 30° and 68° with a dip of about 64–68°. The slip angle on this plane is constrained to lie between 30° and 145°, precluding a strike-slip mechanism and requiring a nearly horizontal compressional axis whose azimuth is restricted to the NW and SE quadrants. Event C_2, on the other hand, produced dilatational arrivals at Abeche, Chad (ABC), La Paz, Bolivia (LPB), and Charters Towers, Australia (CTA). The observation of a compression at Adelaide (ADE), not far from CTA, strongly constrains one of the nodal planes. The data are consistent with a strike-slip mechanism on a nearly vertical fault.

We are in the process of gathering seismograms for other events in Region C. The few first motions we have obtained for the two events of October 31, 1977, and July 13, 1978, are all compressional.

The parameters of the fault-plane solutions are listed in Table 5, and their compressional and tensional axes are plotted in Figure 12. The compressional axes all lie in the NW or SE quadrants and the tensional axes all lie in the NE or SW quadrants. Only one nodal plane is given for event C_1; a second plane could be placed with a strike of 164° and a dip of 63°, yielding compressional and tensional axes with strikes of 114° and 22° and dips of 03° and 37°, respectively. The compressional axis corresponding to this choice would differ from that for C_2 by only 7° in strike and 3° in dip.

The similar orientations of the focal mechanisms, despite the large distances separating the three source regions, suggests that they are indicative of a regional stress field of approximately constant orientation. In particular, the fact that their compressional axes are nearly horizontal and roughly

TABLE 5. Focal Parameters of Events in Regions A, B, and C

Event	Nodal Planes				*P* Axis		*T* Axis	
	Strike	Dip	Strike	Dip	Strike	Dip	Strike	Dip
A_1	232	85	141	80	97	11	6	4
A_2	241	75	146	73	104	23	13	1
A_3	253	75	159	75	116	21	26	0
A_4	265	80	169	60	131	28	34	13
B_1	84	69	345	68	305	31	214	1
B_2	103	69	3	66	324	33	232	2
B_3	115	63	22	84	335	23	71	14
C_1	62	67	...	...	...	...	...	...
C_2	62	90	152	90	107	0	17	0

All values in degrees, clockwise from north and positive downward.

aligned with the direction of Pacific plate motion, represented by the arrow on Figure 12, is a feature to which we ascribe tectonic significance.

The consistent orientations and shallow dips of the compressional axes found for Regions A, B and C are compatible with the correlations observed by various authors for other oceanic intraplate earthquakes [e.g., *Mendiguren*, 1971; *Sykes and Sbar*, 1973; *Forsyth*, 1973; *Okal*, 1980]. We note, however, that events in Regions A and B are characterized by strike-slip faulting with some normal component, which does not corroborate *Sykes and Sbar*'s [1973] conclusion that thrust faulting predominates in oceanic crust older than 20 m.y.

TECTONIC STRESS

Intraplate vulcanism is directly responsible for some of the seismicity in the South-Central Pacific, specifically at TM4, TM10 and AU5, where active volcanoes have been identified in the bathymetry [*Talandier and Kuster*, 1976; *Johnson*, 1970]. Other seismic localities in the Tahiti-Méhétia area may be associated with either magmatic activity at depth or the stresses engendered by volcanic loading of the lithosphere. (The geomorphology of Tahiti [*De Neufbourg*, 1965] shows that the volcano, whose activity ceased about 400,000 years ago, is now tilting about a NW-SE axis. It is interesting to note that the zone of seismicity northeast of Tahiti is on the subsiding flank of the volcanic edifice. At present, however, there is no definite evidence of a causal relationship between this subsidence and the earthquake activity.)

Aside from these specific instances, the causes of seismicity in the South-Central Pacific remain largely a matter of speculation. Nevertheless, certain inferences concerning the active tectonics of this vast intraplate area appear to be warranted. According to our interpretation of the depth-phase data from Regions A, B and C, the largest earthquakes have shallow hypocenters probably confined within the oceanic crust. The conclusion cannot be generalized to cover all seismicity—small events in the TM area have been located at depths as great as 40 km (Table 3)—but it does suggest that at least some of the epicenters may be correlated with, and perhaps controlled by, crustal structures expressed as bathymetric features.

It is surprising, therefore, that so little correlation between seismicity and bathymetry can in fact be documented. For example, with the exception of an isolated event at AU3, none of the recorded activity is distributed along the major fracture zones that cross the study area (Figure 3). Evidently these tremendous scarps, whose vertical relief commonly exceeds 1 km, are not the loci of significant present-day deformations, or, if they are, the deformation is occurring aseismically.

A better correlation is apparent between the seismicity and the positions and trends of the island platforms. As we have already noted, one set of epicenter localities (TU1–TU8) is distributed along the tectonic axis of the Tuamotu Archipelago and its extension into the Line Islands, whereas another (TU9, GB1–GB4) is roughly aligned with the northeastern edge of the Tuamotu platform. The latter includes Region B, the site of some of the largest earthquakes in French Polynesia. These components of the seismicity could possibly be caused by load inhomogeneities associated with the island chains.

On the other hand, much of the seismicity in the South-Central Pacific does not correlate with any major bathymetric features. The two outstanding examples are Regions A and C, which together account for 75% of the recorded seismic energy release. On the charts of *Mammerickx et al.* [1975], the bathymetry in the vicinity of Region C is especially featureless, but, unfortunately, the data coverage in this remote area is very poor (the nearest documented ship track passes 200 km north of the epicenters).

Good bathymetric data are available for Region A, however. The epicenters lie in a regional bathymetric low, flanked to the north and south by the Galapagos and Marquesas Fracture Zones and to the east and west by the Marquesas and Line Islands [*Mammerickx et al.*, 1975]. A detailed bathymetric survey by *Sverdrup and Jordan* [1979] reveals that Region A is characterized by subdued topography. Some of the profiles show disturbed sediments possibly related to recent tec-

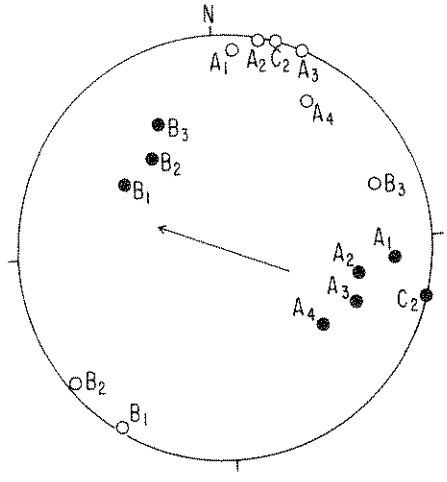

Fig. 12. Stereographic projection of lower focal hemisphere showing *P* axes (solid circles) and *T* axes (open circles) for mechanisms listed in Table 5. Arrow indicates the direction of Pacific plate motion computed at Region B from *Minster and Jordan*'s [1978] model AM1-2 (see Table 6).

TABLE 6. Azimuths of Pacific Plate Motion Computed From Minster and Jordan's Model AM1-2

Locality	Latitude, °S	Longitude, °W	Azimuth: Nazca Plate*	Azimuth: Hotspot Reference Frame†
Region A	7.4	148.3	N61°W	N64°W
Region B	18.4	132.8	N67°W	N69°W
Region C	20.8	127.0	N70°W	N71°W

*Motion with respect to Nazca plate.
†Motion with respect to hotspot reference frame.

tonism, but no major faults and only small (~800 m) seamounts were mapped near the epicentral zone.

Hence, no evidence from either Region A or Region C points to the existence of local bathymetric features which could load the crust or control the direction of faulting. This reinforces our hypothesis, based on the consistent orientations of principal axes seen in Figure 12, that the faulting is indicative of a regional stress field whose orientation is slowly varying over the distances separating Regions A and C (~2000 km).

Turcotte and Oxburgh [1976] and *Richardson et al.* [1979] have reviewed the sources of large-scale lithospheric stress that have sufficient magnitude to fracture rocks (say, greater than 100 bars). Included among these are load inhomogeneities, conductive cooling of the lithosphere, changes in plate curvature due to rigid plate motion on an ellipsoidal earth, and the various forces associated with the driving mechanism of plate tectonics. As we have seen, loading stresses may be locally important to the distribution of some seismicity in French Polynesia, but they do not account for the activity observed in Regions A and C and other localities far removed from major bathymetric features, nor would they be likely to have similar orientations over the spatial scales sampled by the focal mechanisms. Thermal stresses are expected to produce mechanisms whose tensional axes are perpendicular to the age gradient within the plate and therefore perpendicular to the fracture zones [*Turcotte and Oxburgh*, 1976]. Within our study area, this direction is approximately N10°W and is not very consistent with the data in Figure 12. The membrane stresses caused by latitudinal translations on an ellipsoidal earth are more difficult to evaluate, because they depend on the details of the plate geometry as well as its history [*Turcotte*, 1974; *Turcotte and Oxburgh*, 1976]; at present, we have no basis on which to rule out their importance.

However, our preferred hypothesis is to identify the stress field indicated by the focal mechanisms to be the stress deviator imposed by the system of plate-tectonic driving forces. With respect to the Nazca plate or in any of the several 'absolute' reference frames discussed by *Minster and Jordan* [1978], the local plate motions in this part of the Pacific have azimuths between N65°W and N75°W (Table 6). The focal mechanisms from Regions A and C are thus consistent with a tectonic stress deviator whose P and T axes are horizontal and whose P axis is parallel to the plate motion (Figure 12). The Region B mechanisms are somewhat rotated with respect to these principal axes, but, given the uncertainties in the mechanisms and the possibility that the loading stresses in Region B may influence their orientations, the discrepancies cannot be considered significant.

The correlation between the azimuths of compressional axes and the directions of plate motion has been noted elsewhere and attributed to the significance of 'ridge push' in the force balance equation of the plates [*Mendiguren*, 1971; *Forsyth*, 1973; *Sykes and Sbar*, 1973; *Forsyth and Uyeda*, 1975; *Solomon et al.*, 1975; *Richardson et al.*, 1976, 1979; *Okal*, 1980]. Our data are consistent with this inference, and they provide additional constraints on force balance models of the sort discussed by *Richardson et al.* [1979].

DISCUSSION

The available earthquake mechanisms can be satisfactorily explained in terms of a regionally coherent stress field associated with the plate driving mechanism. A homogeneous stress field does not account for the tendency of earthquakes in the South-Central Pacific to be spatially localized into discrete clusters, however. This salient aspect of the seismicity suggests the existence of inhomogeneities within the oceanic crust which act to concentrate stress or to weaken the lithosphere. Stress concentrations or zones of weakness could be the manifestations of heterogeneities frozen into the lithosphere at its time of formation. Alternately, the brittle failure of crustal rocks could be induced by magmatic activity within the crust or at depth. Given the propensity of the area for recent vulcanism and the swarm seismicity at some localities (e.g., Regions A and C), the latter hypothesis has certain attractions, but as yet there exists no corroborating evidence for any magmatic activity away from the previously identified volcanic centers. Whatever the cause of the spatial localization of earthquakes in Region A, for example, it is without obvious expression in the bathymetry [*Sverdrup and Jordan*, 1979].

Acknowledgments. We profited from discussions of intraplate seismicity and vulcanism with H. W. Menard, B. Minster and B. Chouet. We thank J. Schneiderman for her assistance with the data processing, Lamont-Doherty Geological Observatory for the use of their seismogram collection, and the National Geographic Society for permission to reproduce the map in Figure 1. This research was supported by the Office of Naval Research under grants N00014-75-C0152 and N00014-79-C0292 and the Délégation Générale à la Recherche Scientifique et Technique.

REFERENCES

De Neufbourg, G., Notice explicative sur la feuille Tahiti, report Bur. de Rech. Géol. et Min., Paris, 1965.

Duschenes, J. D., and S. C. Solomon, Shear wave travel time residuals from oceanic earthquakes and the evolution of oceanic lithosphere, *J. Geophys. Res., 82*, 1985–2000, 1977.

Forsyth, D., Compressive stress between two mid-ocean ridges, *Nature, 243*, 78–79, 1973.

Forsyth, D., and S. Uyeda, On the relative importance of the driving forces of plate motion, *Geophys. J. R. Astron. Soc., 43*, 163–200, 1975.

Furumoto, A. S., N. N. Nielsen, and W. R. Phillips, A study of past earthquakes, isoseismic zones of intensity, and recommended zones for structural design for Hawaii, *Rep. HIG-73-4*, Hawaii Inst. of Geophys., 1973.

Gutenberg, B., and C. F. Richter, *Seismicity of the Earth and Associated Phenomena*, 2nd ed., Princeton University Press, Princeton, N. J., 1954.

Herron, E. M., Sea-floor spreading and the Cenzoic history of the East-Central Pacific, *Geol. Soc. Am. Bull., 83*, 1671–1692, 1972.

Isacks, B., J. Oliver, and L. R. Sykes, Seismology and the new global tectonics, *J. Geophys. Res., 73*, 5855–5899, 1968.

Johnson, R. H., Active submarine volcanism in the Austral Islands, *Science, 167*, 977–979, 1970.

Johnson, R. H., and A. Malahoff, Relation of Macdonald Volcano to migration of volcanism along the Austral chain, *J. Geophys. Res., 76*, 3282–3290, 1971.

Jordan, T. H., and K. Sverdrup, Teleseismic location techniques and

their application to earthquake clusters in the South-Central Pacific, submitted to *Bull. Seismol. Soc. Am.*, 1980.

Jordan, T. H., K. Sverdrup, E. A. Okal, and J. Talandier, Two seismically active features of the Pacific basin (abstract), *Eos Trans. AGU, 59*, 1135, 1978.

Mammerickx, J., S. M. Smith, I. L. Taylor, and T. E. Chase, Topography of the South Pacific (map), *IMR Tech. Rep. Ser. TR 56*, Scripps Inst. of Oceanogr., Univ. of Calif., San Diego, 1975.

Mendiguren, J. A., Focal mechanism of a shock in the middle of the Nazca plate, *J. Geophys. Res., 76*, 3861–3879, 1971.

Mendiguren, J. A., and F. M. Richter, On the origin of compressional intraplate stresses in South America, *Phys. Earth Planet. Inter., 16*, 318–326, 1978.

Minster, J. B., and T. H. Jordan, Present-day plate motions, *J. Geophys. Res., 83*, 5331–5354, 1978.

Okal, E. A., The Bellingshausen Sea earthquake of February 5, 1977: Evidence for ridge-generated compression in the Antarctic plate, *Earth Planet. Sci. Lett., 46*, 306–310, 1980.

Okal, E. A., and J. Talandier, Rayleigh wave phase velocities in French Polynesia, *Geophys. J. R. Astron. Soc.*, in press, 1980*a*.

Okal, E. A., and J. Talandier, High-frequency Rayleight waves channeled through oceanic sediments following shallow earthquakes in the south-central Pacific Ocean basin (abstract), *Eos Trans. AGU, 61*, 307, 1980*b*.

Orcutt, J. A., and L. M. Dorman, An oceanic long range explosion experiment: A preliminary report, *J. Geophys., 43*, 257–263, 1977.

Richardson, R. M., S. C. Solomon, and N. H. Sleep, Intraplate stress as an indicator of plate tectonic driving forces, *J. Geophys. Res., 81*, 1847–1856, 1976.

Richardson, R. M., S. C. Solomon, and N. H. Sleep, Tectonic stress in the plates, *Rev. Geophys. Space Phys., 17*, 981–1019, 1979.

Richter, C. F., An instrumental earthquake magnitude scale, *Bull. Seismol. Soc. Amer., 25*, 1–32, 1935.

Sakuma, S., and R. Nagata, Physical volcanology, *Handb. Phys., 48*, 982–1011, 1957.

Solomon, S. C., N. H. Sleep, and R. M. Richardson, On the forces driving plate tectonics: Inferences from absolute plate velocities and intraplate stress, *Geophys. J. R. Astron. Soc., 42*, 769–801, 1975.

Sverdrup, K., and T. H. Jordan, Bathymetric survey of seismic region A, South Central Pacific Ocean (abstract), *Eos Trans. AGU, 60*, 957, 1979.

Sykes, L. R., Mechanism of earthquakes and the nature of faulting on the midocean ridges, *J. Geophys. Res., 72*, 2131–2153, 1967.

Sykes, L. R., Earthquake swarms and sea-floor spreading, *J. Geophys. Res., 75*, 6598–6611, 1970.

Sykes, L. R., Intraplate seismicity, reactivation of preexisting zones of weakness, alkaline magmatism, and other tectonism postdating continental fragmentation, *Rev. Geophys. Space Phys., 16*, 621–688, 1978.

Sykes, L. R., and M. L. Sbar, Intraplate earthquakes, lithospheric stresses and the driving mechanism of plate tectonics, *Nature, 245*, 298–302, 1973.

Sykes, L. R., and M. L. Sbar, Focal mechanism solutions of intraplate earthquakes and stresses in the lithosphere, in *Geodynamics of Iceland and the North Atlantic Area*, edited by L. Kristjansson, pp. 207–224, D. Reidel, Hingham, Mass., 1974.

Talandier, J., Etude et prévision des tsunamis en Polynésie Française, Ph.D. thesis, Univ. de Paris, Paris, 1971.

Talandier, J., and M. Bouchon, Propagation of high-frequency P_n waves at great distances in the South Pacific and its implication for the structure of the lower lithosphere, *J. Geophys. Res., 84*, 5613–5619, 1979.

Talandier, J., and G. T. Kuster, Seismicity and submarine volcanic activity in French Polynesia, *J. Geophys. Res., 81*, 936–948, 1976.

Talandier, J., and E. A. Okal, Human perception of *T* waves: The June 22, 1977 Tonga earthquake felt on Tahiti, *Bull. Seismol. Soc. Amer., 69*, 1475–1486, 1979.

Turcotte, D. L., Membrane tectonics, *Geophys. J. R. Astron. Soc., 36*, 33–42, 1974.

Turcotte, D. L., and E. R. Oxburgh, Mid-plate tectonics, *Nature, 244*, 337–339, 1973.

Turcotte, D. L., and E. R. Oxburgh, Stress accumulation in the lithosphere, *Tectonophysics, 35*, 183–199, 1976.

Wesnousky, S. G., and C. H. Scholz, The craton: Its effects on the distribution of seismicity and stress in North America, *Earth Planet. Sci. Lett., 48*, 348–355, 1980.

(Received March 26, 1980;
revised June 23, 1980;
accepted June 25, 1980.)